ΠΑΝΕΠΙΣΤΗΜΙΟ ΚΡΗΤΗΣ
UNIVERSITY OF CRETE

“Morphological and Functional Characterization of Cortical Interneurons in Transgenic mice”

Iason Sifakis

A thesis presented for the Master of Science degree

Graduate Program: Neuroscience

Labaratory of Basic Neuroscience

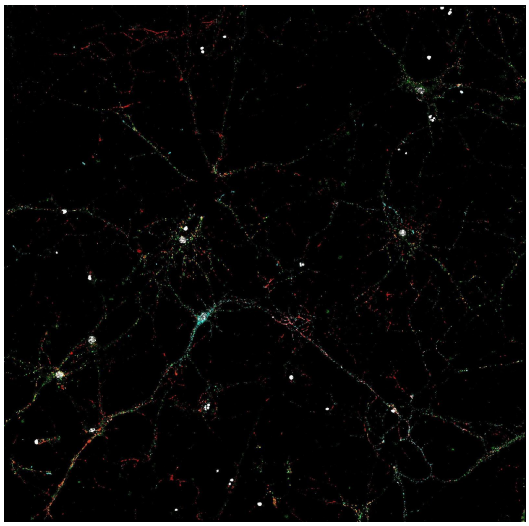

Group Leader: Prof. Domna Karagogeos

University of Crete, Faculty of Medicine, Greece, 2023

ΠΑΝΕΠΙΣΤΗΜΙΟ ΚΡΗΤΗΣ
UNIVERSITY OF CRETE

“ΜΟΡΦΟΛΟΓΙΚΟΣ ΚΑΙ ΛΕΙΤΟΥΡΓΙΚΟΣ ΧΑΡΑΚΤΗΡΙΣΜΟΣ ΕΝΔΟΝΕΥΡΩΝΩΝ ΤΟΥ ΕΓΚΕΦΑΛΙΚΟΥ ΦΛΟΙΟΥ ΣΕΔΙΑΓΩΝΙΔΙΑΚΟΥΣ ΜΥΕΣ”

Ιάσων Σηφάκης

Μεταπτυχιακή Εργασία

Πρόγραμμα Μεταπτυχιακών Σπουδών: Νευροεπιστήμες

Εργαστήριο Βασικών Νευροεπιστημών

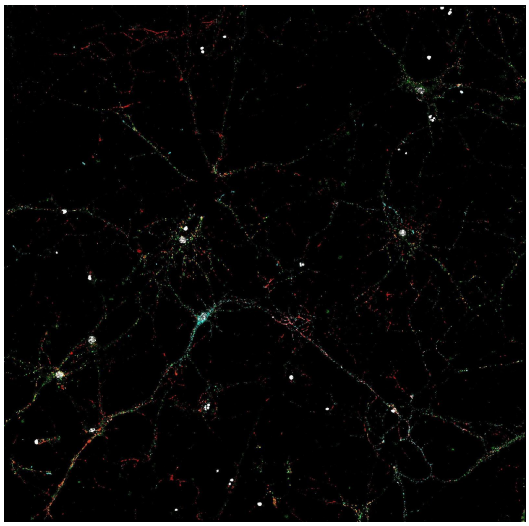

Υπεύθυνος Καθηγητής: Καθ. Δόμνα Καραγωγέως

Πανεπιστήμιο Κρήτης, Τμήμα Ιατρικής, Ελλάδα, 2023

Examination Committee

Domna Karagogeos

Professor of Molecular Biology-Developmental Neurobiology, School of Medicine, University of Crete

Sidiropoulou Kiriaki

Associate Professor, Dept. of Biology, University of Crete

Prof. Vidaki Marina

Assistant Professor of Cellular and Molecular Biology, School of Medicine, University of Crete

Acknowledgment

As I'm coming to the end of this big journey there are a lot of people that I want to thank for their help and support throughout my master's thesis and even more.

Firstly I would like to thank Professor Karagogeos for giving me this big opportunity to be a member of her lab, where I had the chance to learn as much as possible and to develop as a scientist. Also, I would like to thank her for her help and tips in this whole process regarding my thesis and my future as well.

Also, I would like to thank the two people from the lab, who even though they were my supervisors I would also like to consider them friends. First I want to thank Ilias Kalafatakis, who in the three months that we worked together mainly taught me to believe in myself and to start chasing my dreams. Even though he is a Panathinaikos fan, I always enjoyed spending time with him, inside and outside the lab and I would cherish these times in the future. Secondly, I want to thank Sofia Petsagkouraki, who taught me a lot and pushed me to become a better researcher and gain confidence in my skills. I really liked talking with her about our plans and the future and I'm sure the future would be bright for her.

Furthermore, I want to thank other people from the lab as well, especially my best friend Despoina Kaffe, with whom we started our journey and friendship together during our bachelor's and continued it throughout our master's. I would really miss spending time with her in the lab and working together. She was always there for me and I am grateful for it. I would also like to thank Athanasia Voulgari who we work together with and consider her as a friend as well. Finally, I would also like to thank Kostas Theodorakis, Nikki Ktena, and Stefanos Kaplanis for the guidance, tips, and eagerness to teach me at every opportunity.

I would also like to thank Sofia Pasadaki from Professor Vidaki's lab, who taught me most of the things I know and was always there to answer my questions. I want to thank Lida Vagiaki and Zoi Drakaki from Professor Sidiroolou's lab, who helped me with the LTP recordings and stayed until late for a week in order to perform them. Finally, I would like to thank Professor Vidaki and Professor Sidiropoulou as well, as they helped this thesis to become possible with their advice and solutions to various problems that we faced.

Also, I would like to thank all of my friends who helped me take my mind off the lab and the experiments, even though some of them couldn't understand why I was in the lab most Sundays. Especially I want to thank my girlfriend who was there for me and believed in me throughout my master's and helped me see the brighter side of each day.

Finally and most importantly I want to thank my family, especially my parents, who have supported me all this time and given me the opportunity to focus on my studies. They were always there for me and believed in me in times and situations when I had really lost hope.

Abstract

Cortical interneurons (CINs), despite constituting a minority of cortical neurons, play critical roles in cortical function and have been implicated in neurological disorders. CINs exhibit remarkable diversity in morphology, molecular markers, and function, reflecting the complexity of their development. This thesis explores the role of the small GTPase Rac1 in the maturation of CINs, with a specific focus on somatostatin-expressing (SST+) CINs and the role of TAG-1/CNTC-2 in the myelination of SST+ CINs and their functions.

Using a genetically engineered mouse model with Rac1 selectively ablated in medial ganglionic eminence (MGE)-derived CINs, we investigated the morphological changes during early postnatal development. Notably, we observed a significant reduction in the soma perimeter of SST+ CINs, suggesting a role for Rac1 in cytoskeletal dynamics. Additionally, we assessed synapse formation in these CINs. Immunocytochemistry revealed a decrease in both inhibitory and excitatory synapse density on the soma and primary dendrites of SST+ CINs lacking Rac1.

Given the extensive connections between pyramidal cells and SST+ interneurons, we propose further investigations into potential alterations in synapses on pyramidal cells in Rac1-deficient mice. While Rac1's involvement in CIN development is well-documented, its precise role in modulating the morphology and synaptogenesis of SST+ CINs during early postnatal stages adds a new layer of complexity. Potential downstream molecules and differential effects in distinct neuronal populations warrant further exploration.

Regarding the TAG-1/CNTC-2 mouse line, electrophysiological recordings show altered potentiation of the CA1 circuit, where our findings reveal a stark difference between TAG-1/CNTN-2 knockout and wild-type animals, suggesting the involvement of intricate inhibitory-excitatory interactions and potential variations in NMDA receptor function.

This thesis offers a comprehensive journey into the world of CINs, unraveling their complex development and functional significance. The insights gained not only expand our understanding of neural circuitry but also open avenues for further exploration into the molecular mechanisms that underlie cortical function.

Keywords: Interneurons, development, Knx2.1, Rac1, synapses, morphology

Abstract (Ελληνικά)

Οι ενδονευρώνες του φλοιού (CINs), παρά το γεγονός ότι αποτελούν την μειονότητα των νευρώνων του φλοιού, παίζουν κρίσιμους ρόλους στη λειτουργία του φλοιού και έχουν εμπλακεί σε νευρολογικές διαταραχές. Τα CIN παρουσιάζουν αξιοσημείωτη ποικιλομορφία στη μορφολογία, τους μοριακούς δείκτες και τη λειτουργία, αντανακλώντας την πολυπλοκότητα της ανάπτυξής τους. Αυτή η διατριβή διερευνά το ρόλο της GTPase Rac1 στην ωρίμανση των CINs, με ιδιαίτερη έμφαση στα CIN που εκφράζουν τη σωματοστατίνη (SST+) και το ρόλο της TAG-1/CNTC-2 στη μυελίνωση των SST+ CINs και τις λειτουργίες τους.

Χρησιμοποιώντας ένα γενετικά τροποποιημένο μοντέλο ποντικού με Rac1 που έχει αφαιρεθεί επιλεκτικά σε CIN που προέρχονται από την έσω γαγγλιακή υπεροχή (MGE), διερευνήσαμε τις μορφολογικές αλλαγές κατά την πρώιμη μεταγεννητική ανάπτυξη. Συγκεκριμένα, παρατηρήσαμε μια σημαντική μείωση στην περίμετρο του σώματος των SST+ CINs, υποδηλώνοντας έναν σημαντικό ρόλο της Rac1 στη δυναμική του κυτταροσκελετού των ενδονευρώνων αυτών. Επιπλέον, με την χρήση ανοσοκυτταροχημείας ανακαλύψαμε μείωση τόσο στην ανασταλτική όσο και στην διεγερτική πυκνότητα των συνάψεων στο σώμα και στους πρωτογενείς δενδρίτες των SST+ CIN που στερούνται Rac1.

Δεδομένων των εκτεταμένων συνδέσεων μεταξύ πυραμιδικών κυττάρων και ενδονευρώνων SST+, προτείνουμε περαιτέρω έρευνες για πιθανές αλλαγές σε συνάψεις σε πυραμιδικά κύτταρα σε ποντικούς με έλλειψη Rac1. Ενώ η συμμετοχή της Rac1 στην ανάπτυξη CIN είναι καλά τεκμηριωμένη, ο ακριβής ρόλος της στη διαμόρφωση της μορφολογίας και της συναπτογενεση των SST+ CINs κατά τα πρώιμα μεταγεννητικά στάδια προσθέτει ένα νέο επίπεδο πολυπλοκότητας. Πιθανά downstream μόρια και διαφορικές επιδράσεις σε διακριτούς νευρωνικούς πληθυσμούς δικαιολογούν περαιτέρω διερεύνηση.

Όσον αφορά τη γραμμή ποντικιού TAG-1/CNTC-2, οι ηλεκτροφυσιολογικές καταγραφές δείχνουν αλλοιωμένη ενίσχυση του κυκλώματος της CA1 του ιπποκάμπου, όπου τα ευρήματά μας αποκαλύπτουν μια έντονη διαφορά μεταξύ TAG-1/CNTN-2 νοκ-άουτ και άγριου τύπου ζώων, υποδηλώνοντας τη συμμετοχή περίπλοκων ανασταλτικών -διεγερτικές αλληλεπιδράσεων και πιθανές αλλαγές στη λειτουργία του υποδοχέα NMDA.

Αυτή η διατριβή προσφέρει ένα ολοκληρωμένο πλάνο στον κόσμο των CIN, αποκαλύπτοντας την πολύπλοκη ανάπτυξη και τη λειτουργική τους σημασία. Οι γνώσεις που αποκτήθηκαν όχι μόνο επεκτείνουν την κατανόησή μας για τα νευρωνικά κυκλώματα αλλά ανοίγουν επίσης επιπλέον δρόμους για περαιτέρω διερεύνηση στους μοριακούς μηχανισμούς που διέπουν τη λειτουργία του φλοιού.

Keywords: Interneurons, development, Knx2.1, Rac1, synapses, morphology

Contents

Introduction

Classification of Cortical Interneurons (CINs)

In the murine cerebral cortex, neurons can be categorized into two main types: pyramidal cells and interneurons, each serving distinct functions in neural circuitry. Pyramidal cells exert their excitatory activity by releasing the neurotransmitter glutamate, facilitating the transmission of information within and between cortical regions and non-cortical structures [1,2]. On the other hand, interneurons release the inhibitory neurotransmitter γ-aminobutyric acid (GABA), acting as a protective mechanism against excessive excitation and contributing to network coordination by inhibiting the activity of target cells and reducing their likelihood of firing. The balance between excitatory pyramidal neurons (PNs) and inhibitory cortical interneurons (INs) drives the modulation of cortical excitatory and inhibitory synapses within local circuits [1,2].

Cortical interneurons (INs) represent a diverse group of neurons projecting locally and profoundly shaping neural network function across the brain. Maintaining an appropriate balance between glutamate and GABA signaling is crucial for the proper development and function of the brain, and dysregulation in this system has been implicated in neurodevelopmental disorders [3]. Despite constituting only about 20% of all cortical neurons, GABAergic interneurons play a significant role in cortical function and have been linked to severe disorders such as schizophrenia, epilepsy, and autism spectrum disorders [2,4].

Cortical interneurons (CINs) exhibit remarkable heterogeneity, displaying diversity in their morphology, molecular profile, and functional characteristics [5,6]. Despite this complexity, there are established criteria for classifying them into distinct subclasses based on various features, such as their morphological structure, neurochemical composition, electrophysiological properties, and their synaptic partners. Moreover, the expression of specific markers plays a significant role in categorizing CINs into subtypes. Notably, CINs can be categorized into three distinct and non-overlapping groups based on the expression of parvalbumin (PV), somatostatin (SST), or the serotonin receptor 5HT3a (5HT3aR) [7,8] (Figure 1A). These classification criteria provide valuable insights into the diversity and organization of cortical interneurons, aiding in the understanding of their roles in neural circuits and their potential implications in various neurological and neuropsychiatric conditions.

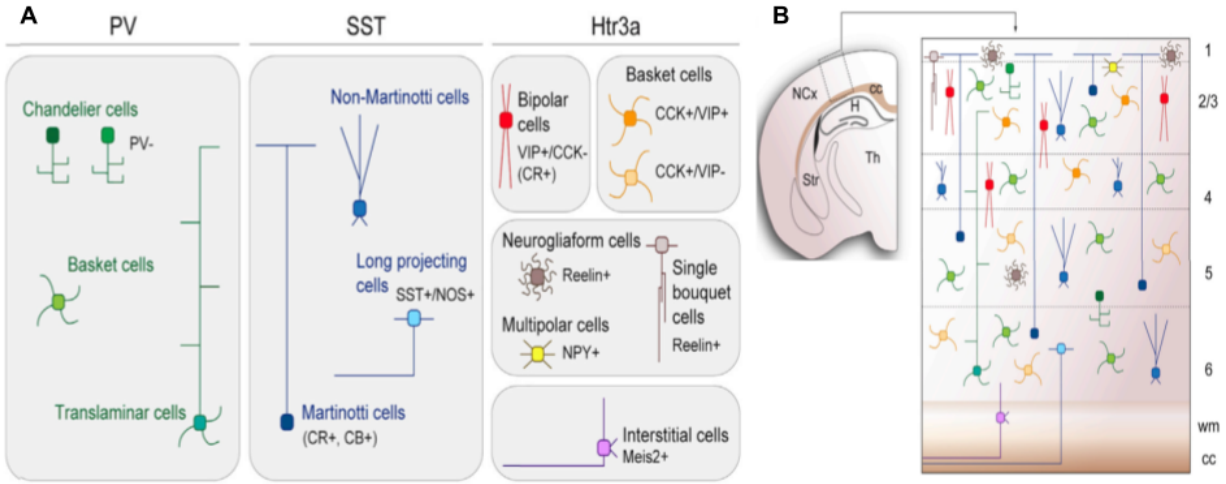

Figure 1. Schematic representation of CINs classes in the mouse neocortex and their distribution on the different layers of the cortex [9].

(A) Classification of GABAergic CINs based on their expression of markers; PV, SST, and the serotonin receptor 3A (Htr3a)

(B) Distribution of PV+, SST+, and 5HT3aR+ INs in cortical layers(Numbers represent the specific layer of cerebral cortex in which CINs can be found. Noticeably, PV basket cells are more abundant than other CINs and are located in most layers of the cortex)

PV interneurons (INs) constitute the principal class of GABAergic inhibitory neurons in the brain and are characterized by their expression of the Ca^{2+} binding protein parvalbumin. This class encompasses three distinct subtypes: basket cells, chandelier cells, and translaminar interneurons. While all three subtypes share the characteristic of fast-spiking firing properties, they diverge in terms of their morphology and synaptic connectivity, underlining this way their unique functional roles [10]. The significance of PV INs lies in their essential role in regulating neural activity. They establish connections with pyramidal cells, playing a crucial part in modulating cortical circuit dynamics [11,12]. Particularly, GABAergic fast-spiking PV interneurons are pivotal in generating cortical oscillations in the gamma frequency range (~30 – 120 Hz). These gamma oscillations play a crucial role in inhibiting large pyramidal cell ensembles and have been implicated in a wide range of cognitive functions, including attention and working memory [13–15]. The importance of gamma synchrony in various cognitive processes highlights the significance of PV INs in the proper functioning of the brain. Additionally, abnormalities in gamma oscillations have been well-documented in schizophrenia, providing insights into potential mechanisms underlying this neuropsychiatric disorder [16].

Basket cells, one of the prominent subtypes of PV+ interneurons, constitute a substantial fraction of cortical inhibitory neurons. They are distributed across all six cortical layers, except for layer 1 (Figure 1B). Basket cells establish synapses on the soma and proximal dendrites of pyramidal cells as well as other types of interneurons, contributing to the modulation of cortical circuit activity [17]. Chandelier cells, distinguished by their chandelier-like morphology, are

predominantly situated between cortical layers 1 and 2 and in layer 6 (Figure 2). Notably, they exhibit a distinct pattern of synaptic connectivity by targeting the axon initial segment of pyramidal cells, playing a crucial role in regulating the initiation of action potentials [18].

Lastly, a relatively rare subset of PV+ interneurons is represented by translaminar interneurons. These specialized cells are specifically localized in cortical layers 5 and 6, as illustrated in Figure 2. Similar to basket and chandelier cells, translaminar interneurons also establish connections with pyramidal cells, contributing to the fine-tuning of cortical network activity [19,20].

The diverse distribution and synaptic targeting of these PV+ interneuron subtypes highlight their significance in shaping cortical circuitry and influencing neural dynamics. Understanding the distinct roles of basket-, chandelier-, and translaminar-interneurons adds to our comprehension of cortical function and may hold implications for investigating various brain disorders and cognitive processes.

The second class of GABAergic cortical interneurons (CINs) is characterized by the expression of the somatostatin (SST) neuropeptide. SST-expressing INs exhibit further subcategorization into three distinct types: Martinotti cells, non-Martinotti cells, and long-projecting cells (Figure 1A). The non-Martinotti cells, despite their considerable heterogeneity, share a common morphological feature - an ascending axon that branches extensively within cortical layer 1 [21–23]. Martinotti cells are primarily distributed across layers 2, 3, and 5 [24,25], and they often play a role as mediators of disynaptic inhibition within the cortical circuitry [26]. On the other hand, non-Martinotti cells are found throughout layers 2 to 6, with a notably abundant presence in layer 4, where they establish connections with PV+ basket cells [27] (Figure 1B).

The third subtype, long projecting cells, predominantly resides in the deep layers of the cortex and projects to other regions within the neocortex. These cells display unique spiking properties characterized by adapting and irregular firing. Additionally, long-projecting cells often co-express nitric oxide synthase (NOS), chondrolectin (Chodl), and neuropeptide Y (NPY) [9].

The diversity of SST-expressing CINs, with distinct morphologies and synaptic connectivity patterns, underscores their vital roles in shaping cortical circuit dynamics and influencing various neural processes. Understanding the specific functions and contributions of Martinotti, non-Martinotti, and long-projecting cells provides valuable insights into the complex organization and functioning of the neocortex and its implications for brain function and pathology.

The final main group of GABAergic CINs expresses the serotonin receptor 5HT3aR (Figure 1A). This diverse group primarily consists of vasoactive intestinal peptide (VIP)+ cells. Notably, these INs predominantly target PV+ and SST+ cells, making them commonly known as disinhibitory cells [24]. They are primarily situated in cortical layers 2 and 3 (Figure 1B). The 5HT3aR+ CINs exhibit two distinct morphological types - bipolar or multipolar basket cells. The latter group encompasses VIP- interneurons, which establish synapses on the soma of pyramidal cells and other interneurons, further contributing to cortical network dynamics [28]. Within the 5HT3aR+ category, there are additional subtypes, including neurogliaform cells. These cells are characterized by late spiking firing properties and facilitate volumetric GABA transmission, thereby influencing cortical inhibitory networks [29]. Transcriptionally similar to neurogliaform cells are the single bouquet cells, both of which are enriched in cortical layer 1

(Figure 1B) [30]. Furthermore, the 5HT3aR+ INs also encompass NPY+ multipolar cells and Meis2+ interstitial INs. NPY+ multipolar cells are located between layers 1 and 2, while Meis2+ interstitial INs extend from the white matter to deeper cortical layers (Figure 1B) [31,3233].

The diverse array of 5HT3aR+ CINs, exhibiting different firing properties and synaptic connectivity patterns, underlines their significant roles in modulating cortical circuitry and shaping neural activity. Understanding the distinct characteristics and functions of these subtypes provides valuable insights into the complexity of cortical inhibitory networks and their impact on cortical function and behavior.

To summarize, the diversity of interneurons in the cerebral cortex plays a crucial role in modulating neuronal activity and maintaining a balance between excitation and inhibition. These specialized cells contribute to the precise regulation of cortical circuits, influencing various cognitive functions and their dysregulation has been implicated in several neurological and neuropsychiatric disorders.

Development and Differentiation of Cortical Interneurons

The identity of cortical inhibitory neurons (CINs) is intricately shaped by their origin and the dynamic changes occurring during their maturation. Specifically, all CINs originate from progenitor cells situated in subpallium structures of the embryonic telencephalon known as ganglionic eminences. Subsequently, these cells undergo tangential and radial migration to attain their final positions within the developing cortex [1,34,35]. The process of laminar allocation, involving radial migration, precedes a crucial phase known as wiring, during which dendritic and axonal morphogenesis takes place, and synapses are established (Figure 2A). As part of the subsequent developmental stage, a fraction of CINs undergo programmed cell death, followed by circuit refinement [36].

Cortical interneurons (CINs) undergo a complex process of development, starting from their generation in the subpallium (ventral telencephalon), followed by tangential migration and subsequent radial migration to their final destinations within the layers of the cerebral cortex. During this maturation phase, they acquire their distinctive morphological and synaptic properties, becoming functionally active components of cortical circuits [6,37,38]. The subpallial origin of CINs in both rodents and primates exhibits remarkable complexity, with multiple progenitor domains characterized by unique combinations of transcription factors, thus governing the fate of cortical interneurons. These domains, including the lateral ganglionic eminence (LGE), medial ganglionic eminence (MGE), caudal ganglionic eminence (CGE), preoptic area (POA), preoptic-hypothalamic (POH) border domain, and septum, play crucial roles in the generation of CINs (Figure 2B) [39]. The expression of the transcription factor Nkx2.1 in the ventral subpallium prior to MGE neurogenesis marks the regional identity and imparts distinct characteristics to progenitor cells in this domain, setting them apart from those in other subpallial regions [40]. The heterogeneity of CINs is reflected in the various types generated from different regions (Figure 2C). Among these, the majority (approximately 60%) are derived from the MGE and subsequently differentiate into parvalbumin (PV) or somatostatin

(SST)-expressing interneurons (Figure 2C). This intricate process of subpallial specification and differentiation contributes to the remarkable diversity of cortical interneurons, each playing specialized roles in shaping cortical circuitry and regulating cortical activity [41–45].

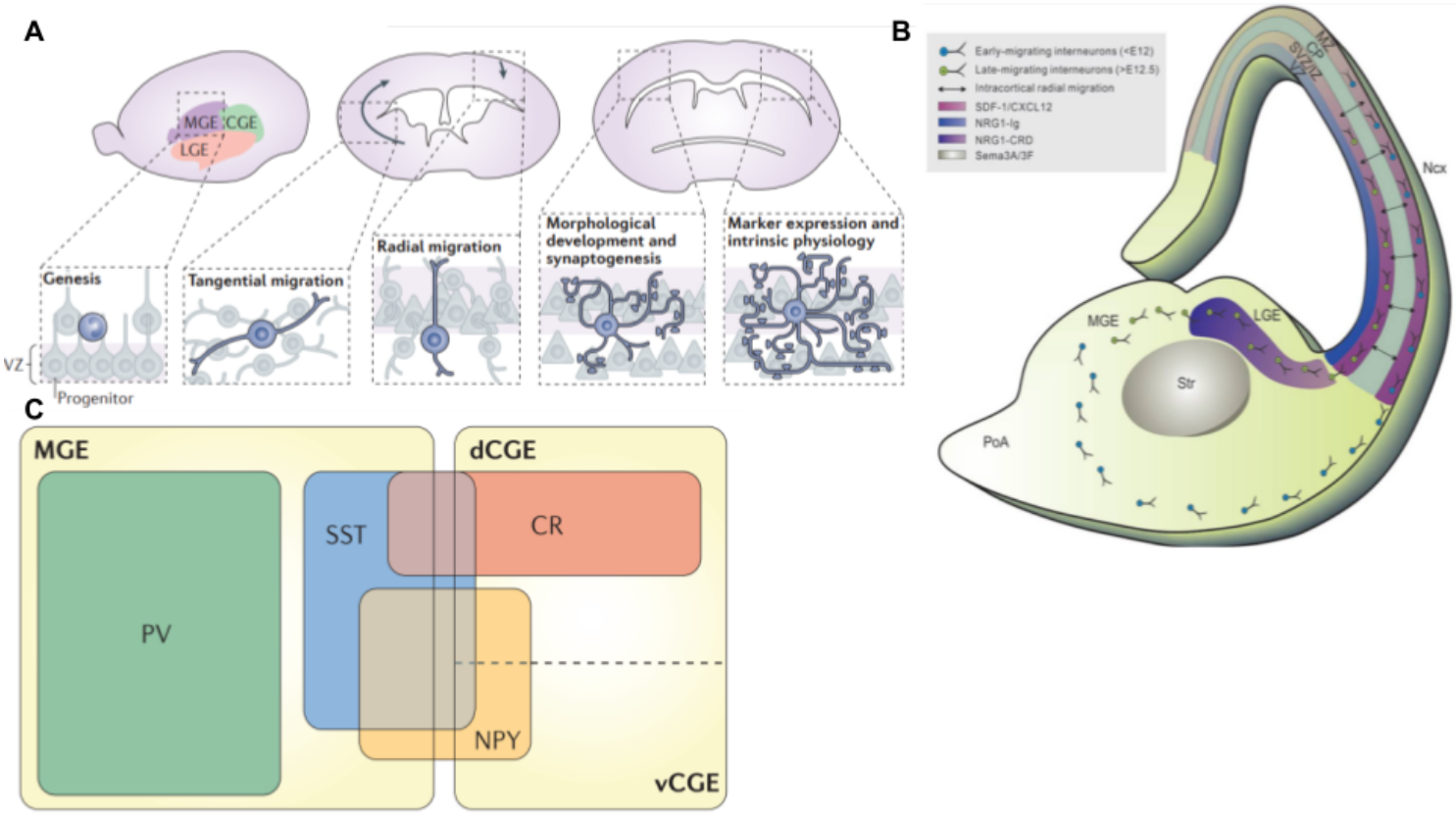

Figure 2: Schematic presentation of the development, differentiation, and migration of the CINs. Classification of GABAergic CINs based on their expression of markers; PV, SST, and the serotonin receptor 3A (Htr3a)

A) The milestones during the development of the CINs [36].

B) Origin and tangential migration of neocortical interneurons [46]. CINs progenitors originate from distinct ganglionic eminences, undergoing tangential migration to enter the cortex. During migration, early INs (shown in blue) traverse the marginal zone (MZ) superficially, while a second, more prominent cohort (INs in green) migrates deeply through the lower intermediate zone (IZ) and subventricular zone (SVZ).

C) Relative contributions of the MGE and CGE to cortical interneuron neurochemical subgroups [47]. Parvalbumin (PV)-expressing interneurons are predominantly derived from the medial ganglionic eminence (MGE), while somatostatin (SST)-containing interneurons are primarily generated in the MGE with potential contributions from the ventral caudal ganglionic eminence (vCGE) and dorsal CGE (dCGE). Neuropeptide Y (NPY)-expressing interneurons mainly originate from the vCGE and dCGE, while calretinin (CR)-containing interneurons are primarily derived from the dorsal CGE (dCGE).

Mechanisms Regulating Cortical Interneuron Diversity

The intricate diversity of interneurons becomes evident during the various stages of their embryonic development. This remarkable diversity is attributed to specific transcriptional programs within the progenitor cells of interneurons, which are responsible for regulating their molecular characteristics and fate [1,48]. These transcriptional programs can be intrinsically encoded within the cells or influenced by interactions with the surrounding microenvironment during development, as illustrated in Figure 3. Notably, one key player at the forefront of the molecular cascade governing the development of parvalbumin (PV) and somatostatin (SST) interneurons is the transcription factor Nkx2.1, whose expression begins at embryonic day 9 (E9) (Figure 3) [49].

Molecules Regulating Cortical Interneuron's Development

The guidance of interneurons (INs) from their subpallial origins to the cortex is facilitated by a complex interplay of extracellular signals, including attractive and repulsive factors, surface-bound permissive and instructive molecules, and mitogenic factors [1,40,48]. While many extracellular signals involved in this process have been identified, our understanding of the intracellular proteins that mediate the cellular response to these cues remains limited [50]. However, emerging research has implicated Rac1, a ubiquitously expressed member of the Rho-GTPase family, as a key intracellular component involved in INs development [51]. Rho-GTPases, including Rac1, play crucial roles in various cellular functions, such as the regulation of actin dynamics, cell cycle, the establishment of polarity, and axonogenesis [51–54]. Perturbations in the regulation and function of these proteins have been linked to cognitive impairments [55,56]. Specifically, alterations in Rac1 activity have been associated with defects in several stages of INs development, including migration, neurite extension, branching, and the establishment of cortical circuits.

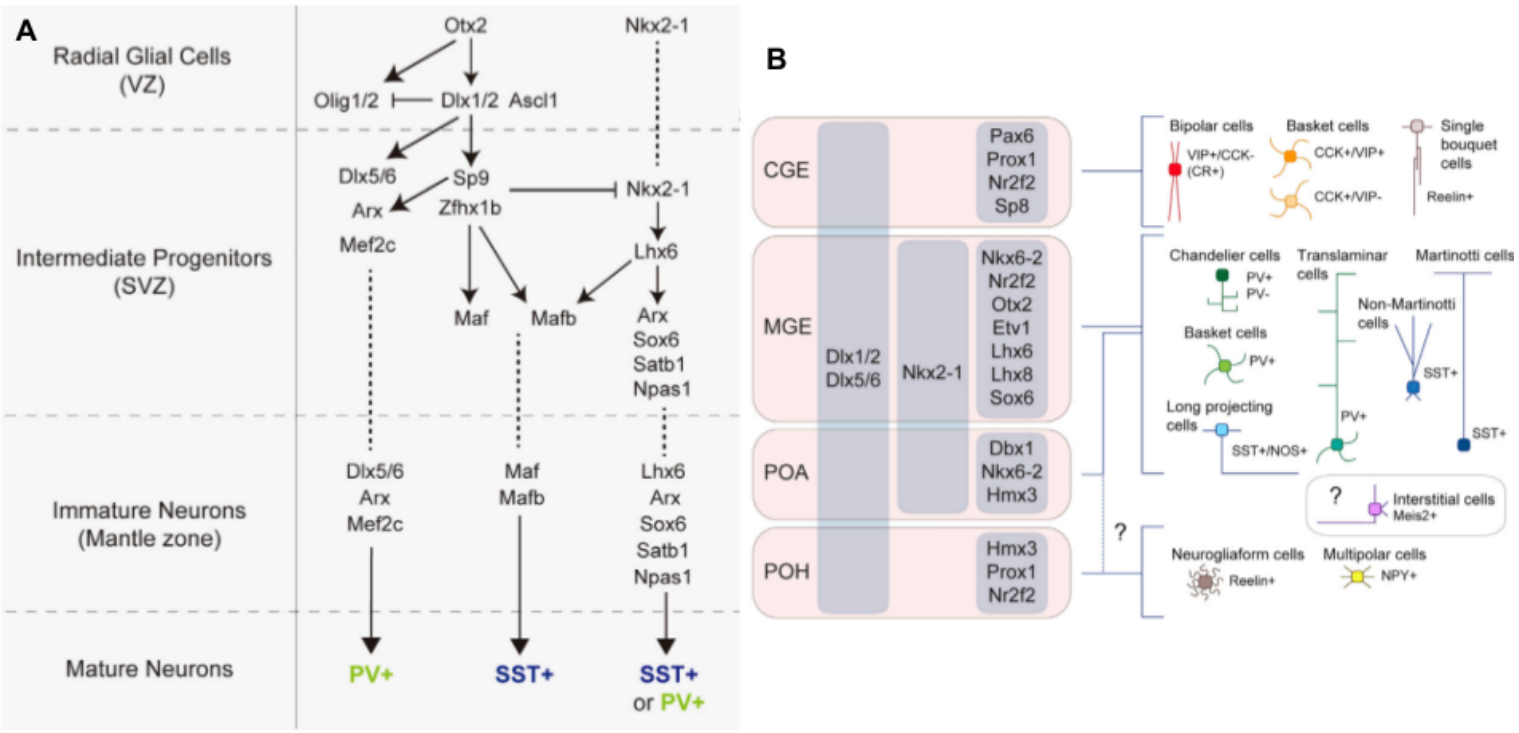

Figure 3. The genetic program regulating the maturation of CINs [9] The diversification of cortical interneurons is largely attributed to variations in transcriptional programs within progenitor cells, starting from the early stage of Radial Glial cells and continuing until progenitors differentiate and acquire the characteristics of mature interneurons.

Rac1 Affects Cortical Interneurons Migration and Morphology

Apart from its effects on CINs migration, emerging evidence suggests that Rac1 plays a pivotal role in regulating the morphological development of these interneurons. Specifically, targeted deletion of Rac1 from MGE-derived INs results in altered cellular morphology [57]. The Rac1-deficient INs exhibit impaired migration towards the cortex, leading to their accumulation in the ventral telencephalon. Furthermore, these cells display notable abnormalities in their growth cones, which are essential for axonal guidance and neurite outgrowth, and consequently, their neurite length is significantly shorter compared to control cells [58]. These findings align with previous studies that have highlighted the importance of Rac1 in regulating cytoskeletal dynamics, which are critical for cell shape and structural plasticity. The observed alterations in Rac1-deficient INs provide valuable insights into the intricate molecular mechanisms that govern

the proper development of cortical interneurons and underscore the significance of Rac1 in orchestrating various aspects of their maturation and integration into cortical circuits [53,54,59].

In-depth investigations into the functional role of Rac1 in cortical interneurons were conducted using small interfering RNA (siRNA) to downregulate Rac1 expression in mouse primary hippocampal neurons revealing a significant impact on the morphological characteristics of interneurons [60]. Specifically, Rac1 knockdown led to a notable reduction in the complexity of the dendritic arborization (dendritic tree) of interneurons, rendering them less elaborated compared to control neurons that were transfected with siRNA against luciferase [60].

These findings underscore the critical significance of Rac1 in orchestrating the intricate processes that underlie the morphological and migratory differentiation of cortical interneurons, highlighting its indispensable role in shaping the neural circuitry of the cerebral cortex.

The synaptic formation being affected by Rac1

Rac1 is a master organizer of the actin cytoskeleton, which in turn plays a pivotal role in the formation and function of postsynaptic dendritic spines (Figures 4) [61–66]. These spines serve as crucial sites for anchoring postsynaptic receptors and organizing postsynaptic densities [67,68]. Overexpression of Rac1 in wild-type primary hippocampal neurons has been found to increase the density of dendritic spines, implicating Rac1 in synapse formation [69]. Interestingly, in Rac1/Rac3 double-knockout hippocampal cultures, re-expressing Rac1 is sufficient to induce the formation of mature spines, thereby restoring spinogenesis [69].

Chemical synapses in the brain can be divided into two main categories: the excitatory glutamatergic synapses and the inhibitory GABAergic synapses (Figure 4B) [70,71]. Glutamatergic synapses release glutamate, an excitatory neurotransmitter, from the excitatory presynaptic terminals, which are located on dendritic spines or dendritic shafts. Neurotransmitters are taken up and stored in synaptic vesicles before exocytotic release into the synaptic cleft [72] (Figure 4B). The intricate orchestration of Rac1 in the regulation of dendritic spine morphology and synaptic organization underscores its significant role in shaping the formation of functional neural circuits [61–66].

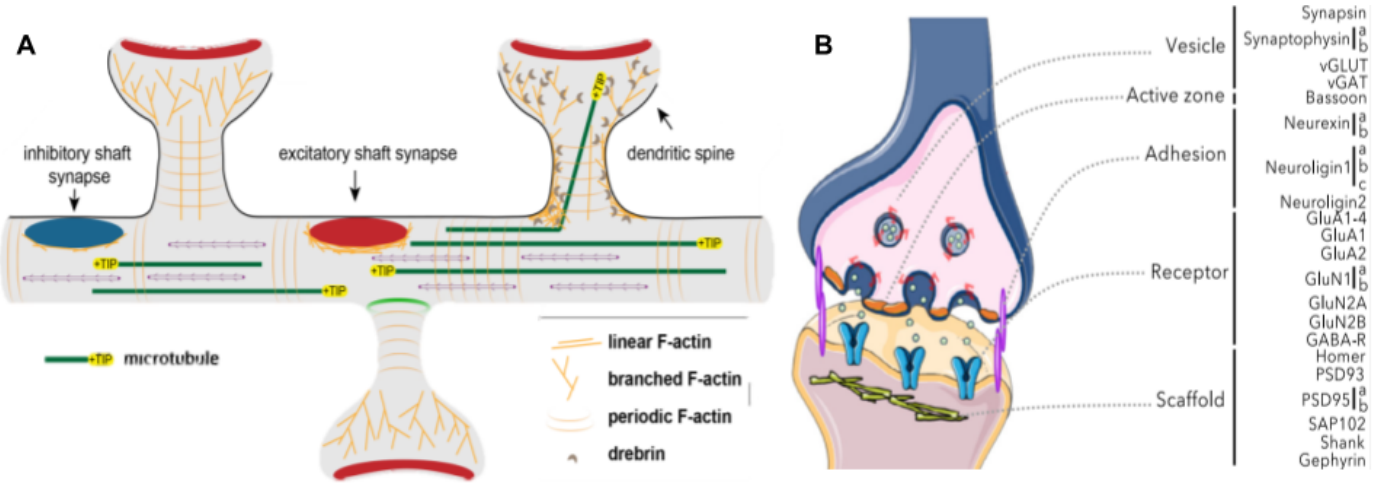

Figure 4 Schematic illustration of synapses and their different markers divided into different categories.

A) Schematic illustration of the cytoskeletal architecture of spines and dendrites [73]. Excitatory synapses are mostly located on dendritic spines and shafts, whereas inhibitory synapses are primarily formed on dendritic shafts and the soma of postsynaptic neurons. Spine and shaft synapses differ in their cytoskeletal components, which provide them with mechanical support.
B) Schematic representation of a typical chemical synapse and list of markers of different functional classes[74].

Postsynaptic density (PSD) represents a critical component in the organization of synapses, consisting of scaffolding proteins associated with cytoskeletal elements that anchor synaptic receptors, ion channels, and adhesion molecules on the postsynaptic cell (Figure 4B). Precise regulation of surface expression, localization, and removal of these components is facilitated by interactions between postsynaptic scaffolds, which have been implicated in synaptic plasticity [75,76]. Among the prominent PSD scaffold proteins in excitatory synapses is PSD-95, a member of the membrane-associated guanylate kinases family (MAGUKs), characterized by their highly organized domains that anchor and cluster synaptic membrane proteins [77,78]. PSD-95 also interacts with F-actin binding proteins, contributing to the structural stability and organization of the PSD (Figure 4A).

Synapsin-1, a member of the synapsin family of phosphoproteins, is a key excitatory synaptic marker that interacts with synaptic vesicles (SV) and the actin cytoskeleton, regulating vesicle trafficking and short-term plasticity [79]. In contrast, inhibitory synapses are primarily formed on the dendritic shaft and soma of neurons, with fewer inhibitory synapses located at spines in the neocortex [80]. GABAergic PSD is predominantly organized by a scaffold protein called Gephyrin, responsible for the localization and number of inhibitory receptors at the synaptic membrane [81–85] (Figure 4B). In general, inhibitory synapses are in closer proximity to

cytoskeletal elements, such as microtubules and intermediate filaments, compared to excitatory spine synapses, suggesting a potentially different mode of interaction with other cytoskeletal components (Figure 4A) [73]. The vesicular GABA transporter (VGAT) plays a crucial role in mediating the accumulation of GABA into synaptic vesicles [86,87] (Figure 4B) and has been widely used as a presynaptic marker for inhibitory synapses. The precise organization and regulation of PSDs and synaptic markers are essential for the proper functioning of neuronal circuits and synaptic transmission.

How Cortical Circuits are Affected by Rac1

Cortical GABAergic interneurons (CINs) play a crucial role in regulating cortical network oscillations and maintaining the balance between excitatory and inhibitory mechanisms in the brain, which is essential for protecting neural tissue from excessive excitation [88,89]. Dysfunctions or loss of CINs have been linked to abnormalities in oscillatory activity, particularly in the gamma frequency range (30-80 Hz), and have been associated with various neuropsychiatric and neurodegenerative disorders, such as autism spectrum disorders, schizophrenia, bipolar disorder, and depression [90–94].

Moreover, alterations in the intracellular signaling protein Rac1, which is involved in regulating cytoskeletal dynamics and dendritic spine formation, have been shown to impact synaptic plasticity in the prefrontal cortex [95]. Studies utilizing Rac1 conditional knockout mice with decreased inhibitory neurons, specifically PV and SST INs, revealed changes in glutamatergic transmission properties of prefrontal cortex neurons. These alterations were characterized by reduced synaptic plasticity, NMDA receptor expression, and dendritic spine density, which were partly restored in the presence of a GABA-A receptor agonist, suggesting a homeostatic mechanism involving GABAergic function [95].

Furthermore, Rac1 deficiency led to increased basal synaptic transmission, spontaneous activity, decreased threshold for stimulus-induced epileptiform activity, and disrupted oscillatory activity in the adult mouse barrel cortex [96]. These findings indicated that reduced GABAergic inhibition not only affected synaptic properties and plasticity but also disrupted neuronal synchronization in the cerebral cortex [96]. Together, these studies emphasize the critical role of Rac1 and GABAergic interneurons in maintaining the proper functioning and synchronization of cortical circuits, with potential implications for understanding the pathophysiology of neurological disorders.

The Connection Between Interneurons and Oligodendrocytes

Oligodendrocytes play a crucial role in the myelination of axons, arising from Oligodendrocyte Precursor Cells (OPCs), which actively sense signals from neighboring neurons through various communication mechanisms. OPCs receive both synaptic and non-synaptic inputs from neurons, leading to functional and phenotypic alterations [97]. Interestingly, OPCs and interneurons share a common origin, primarily derived from distinct ganglionic eminences, with the first wave of OPCs originating from the medial ganglionic eminence (MGE) under the transcriptional control of the Nkx2.1 transcription factor [36,98]. Interneurons, also originating from the ganglionic eminences, display genomic regulation dependent on the Nkx2.1 transcription factor, with a significant portion originating from the MGE, giving rise to parvalbumin (PV) and somatostatin (SST) expressing interneurons [9]. Both MGE-derived interneurons and OPCs exhibit preferences in establishing connections and communication with each other, potentially influencing their interactions during development. Although PV interneurons are observed to connect with OPCs, it does not seem to directly impact intrinsic myelination, as OPCs receive synapses from non-myelinated PV interneurons [99,100]. Nevertheless, their interactions may influence myelination, maturation, and developmental processes. Notably, dysfunctions in PV interneurons and oligodendrocytes have been associated with neurodevelopmental disorders, including schizophrenia, underscoring the intricate relationship between these cell types in the context of neural circuitry and disorders [101].

Recent research teams have unveiled the myelination of numerous GABAergic inhibitory neurons within the cerebral cortex. [99] using the power of light and electron microscopy, revealed an abundance of myelin, predominantly enshrouding layers 2/3 and 4 of the neocortex, intricately associated with interneurons, and more notably the parvalbumin+ basket cell subtype. Intriguingly, this mode of myelination manifests as a discontinuous, patchy-like pattern. Noteworthy departures in protein distribution from their non-GABAergic counterparts surface, with a 20% elevation in the expression of Myelin Basic Protein (MBP) witnessed in GABAergic inhibitory neurons [99]. In contrast, levels of Proteolipid Protein (PLP) exhibit no appreciable discrepancy between the two neuronal populations [102].

Furthermore, the myelination of GABAergic interneurons unfurls as a process inherently contingent upon the brain region. In the CA1 sector, an astonishing 80% of myelin clustered within the stratum pyramidale and stratum radiatum trace their origins to parvalbumin (PV) interneurons [103]. Subsequent investigations by [104] unveiled that within hippocampal PV interneurons residing in the stratum pyramidale of CA1, the adhesion molecule TAG-1 assumes a prominent role, a distinctive presence not mirrored in other strata such as lacunosum-moleculare. Intriguingly, hippocampal cultures disclosed that PV and somatostatin (SST) interneurons accentuate their cellular adhesive repertoire, encompassing the likes of Caspr2 and Kv1 channels, underscoring the intricate molecular ballet of myelination within these neurons' milieu [104]. This intricate interplay between neuronal subtypes and their adhesive molecules augments our comprehension of the diverse landscape of myelination in the cerebral cortex.

The Different Types And The Role Of Myelination

Oligodendrocytes (OLs) are distinct subsets of glial cells within the Central Nervous System (CNS), while Schwann cells perform similar functions within the Peripheral Nervous System (PNS). These cells play a crucial role in supporting neurons and facilitating efficient signal transmission by enveloping axons with myelin—a process known as myelination [105]. The myelin sheath, a lipid-rich, multi-lamellar structure synthesized by OLs in the CNS, serves various essential functions. It facilitates rapid, saltatory propagation of action potentials over long distances, achieved through the concentration of voltage-dependent sodium channels at the nodes of Ranvier [105]. Beyond this, myelin has been recognized for its involvement in fine-tuning neuronal network activity by synchronizing firing patterns [106], while simultaneously providing metabolic support and protective attributes to axons [107].

The process of CNS myelination encompasses two distinct phases: the intrinsic phase and the adaptive phase. The intrinsic phase, genetically determined and fixed in terms of topology and chronology, occurs during birth and early childhood [108]. Oligodendrocyte precursor cells play a pivotal role during this phase by detecting axons eligible for myelination based on morphological characteristics such as axon diameter. The resulting myelin sheath correlates with the calibers of OLs, reflecting their transcriptional programming before differentiation [108].

In contrast, the adaptive phase constitutes the second stage of CNS myelination and involves the modification of pre-existing intrinsic myelin sheaths. This phase is highly plastic, subject to alterations throughout an individual's lifetime through external signaling mechanisms, primarily influenced by neuronal activity [109]. This interaction triggers changes in myelin sheath properties, including their number and size, leading to diverse myelination levels among individuals. Consequently, a "smart wiring" model emerges, whereby already myelinated axons undergo modifications in their myelin sheath thickness (Figure 5E)[109]. This intricate process not only highlights the dynamic nature of myelination but also underscores its fundamental role in shaping neural circuitry and function.

Spatial And Molecular Organization of Myelin

Myelinated axons exhibit intricate organizational specializations, characterized by a precise axonal compartmentalization encompassing distinct domains: nodes of Ranvier, paranodes, juxtaparanodes, and internodes. At the nodes of Ranvier, spanning approximately 1 μm, clusters of voltage-gated sodium channels (Nav) are situated, facilitating saltatory conduction along the myelinated axon [110]. This conduction critically relies on two pivotal phenomena: the formation of myelin sheaths by oligodendrocytes (in the CNS) and the aggregation of Nav channels. This intricate architecture includes key constituents such as Nav, Neurofascin isoforms (Nfasc186 and Nfasc140), Contactin 1 (CNTN1), βIV spectrin, AnkyrinG, and various subtypes of voltage-gated potassium channels (Kv.7), orchestrating its myelination [110].

Adjacent and bilaterally juxtaposed to the nodes of Ranvier, the paranodes constitute the principal site of interaction between oligodendrocytes and the axolemma. This region houses a remarkable intercellular complex, featuring glial Nfasc155, axonal Contactin-associated protein 1 (Caspr, a neurexin family member), axonal CNTN1, ankyrin B, and glial components [111]. The paranodes serve as a barrier between the nodes housing sodium channels and the juxtaparanodes harboring potassium channels, thus preventing nodal currents from traversing the internodes. This crucial barrier formation is essential early in myelination [111].

The juxtaparanodes, part of the internodes, adjoin the paranodes in each myelin structure. Comprising CNTN2/TAG-1 on both axolemma and glia membrane, Caspr2 (CNTN-associated protein 2), and voltage-gated potassium channels, CNTN2/TAG-1 is pivotal for VGKC maintenance in this region. The scaffolding protein 4.1B orchestrates interactions among these molecules, VGKCs, and the cytoskeleton. Depletion of 4.1B coupled with metalloproteases ADAM22/23 disrupts VGKC recruitment, potentially affecting internodal functionality in terms of re-excitation prevention and internodal resting potential preservation [112].

Finally, extending extensively along the perinodal region, internodes represent myelinated territories adjoining juxtaparanodes and nodes of Ranvier. Fundamental components include SynCam molecules, part of the Nectin-like family of adhesion molecules, and immunoglobulin cell adhesion proteins. These entities, which can interface with the cytoskeleton via FERM-binding and PDZ domains, are pivotal for internode regulation, potentially involving interaction with the 4.1B protein (Figure 5A-D) [112]. This intricate spatial and molecular architecture underscores the critical role of myelin in enabling efficient signal propagation and maintaining the integrity of neural circuits.

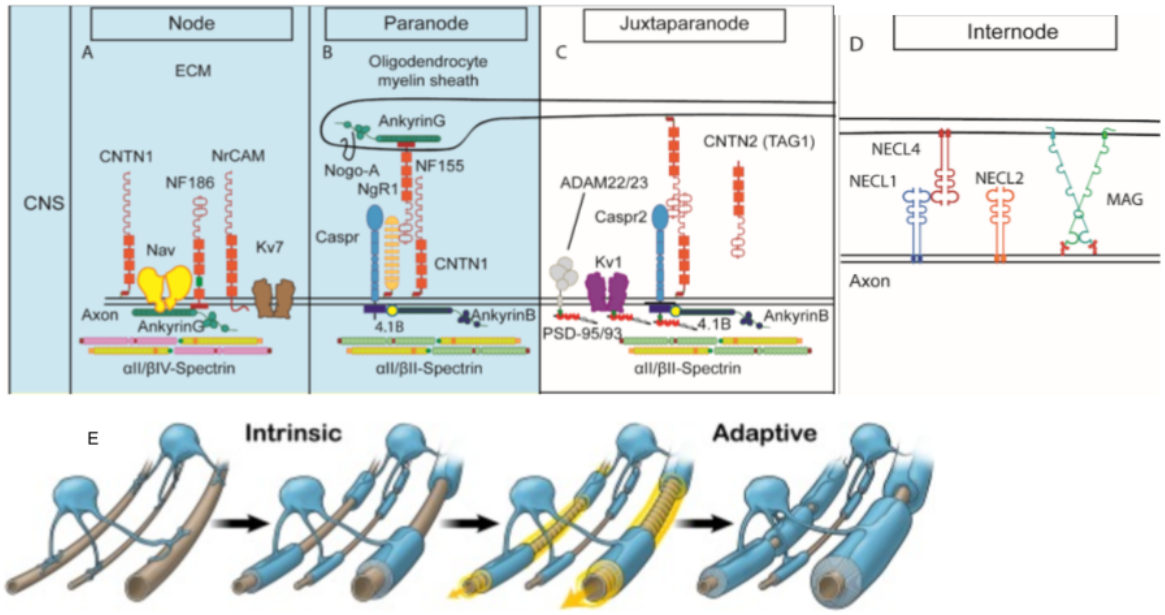

Figure 5: Molecular composition of A) the nodes of Ranvier B) Paranodes C) Juxtaparanodes of the central nervous system (CNS), and Internode. In each myelin domain are depicted all molecules needed for the formation of compartmentalization of the perinodal area [112]. E)

Proposed model from Bechler and colleagues for intrinsic and adaptive myelination in the CNS. They demonstrate sequential intrinsic and adaptive pathways that produce “smart” wiring. This model is correlated to activity and also enables learning, through synaptic plasticity [109].

Aim of the study

This study was a compilation of experiments regarding two different projects. The first project had as the main goal to compare the SST+ interneurons that originate from the MGE between the two mice lines of WT and Rac1-/-; Nkx2.1+/Cre. In the second project, the primary goal was to characterize how TAG-1/CNTN-2 is affecting the synapses and in this specific study, the main focus was on how the absence of TAG-1/CNTN-2 is affecting the synapses on SST+ interneurons.

Regarding the first project, previous studies have implicated Rac1 in the formation of dendritic spines and cortical circuits, yet its involvement in the status of individual CINs remains to be further investigated, especially in a cell type-specific manner. To shed light on this role, we performed in vitro studies, by using a mouse model in which Rac1 is specifically ablated from MGE-derived INs, namely PV and SST INs. In Rac1 cKO mice, only 50% of INs manage to reach the cortex [58], which restricts our study to this group of cells. Following the establishment of primary mixed cortical cultures, we compared the morphological traits of SST INs, such as soma perimeter and dendritic arborization, derived from Rac1 cKO mice to those dissociated from their control littermates. Furthermore, we searched for any differences in inhibitory synapse density on SST-expressing CINs between the two groups of mice. Excitatory synapse density on SST CINs was also assessed for both control and Rac1 cKO mice.

Finally, in the second project, it is known that TAG-1/CNTN-2 plays an important role in the recruitment of the Kiv channels, which can affect the stimulation of the cells and by extension the network. Also, it is known that some types of interneurons(PV+ and SST+) are myelinated. So we wanted to see how TAG-1/CNTN-2 can affect the excitability of the SST+ interneurons. We performed electrophysiological recording of the CA1 area of the hippocampus to see any difference in the excitability.

Materials and Methods

Animals

Rac1

Mice carrying a floxed allele of Rac1 (Rac1fl/fl; Nkx2.1+/Cre) were previously characterized (Reference 64). Specifically, mice carrying a floxed allele of Rac1 (Rac1fl/fl), wherein the 4th and 5th exons of the Rac1 gene are flanked with loxP sites [113], were bred with Nkx2.1Tg(Cre) mice (Nkx2.1 transgenic Cre;[114]), resulting in the Rac1fl/fl; Nkx2.1Tg(Cre) genotype. Additionally, the ROSA26fl-STOP-fl-YFP allele was introduced as an independent marker [115] to visualize and potentially trace MGE-derived INs (Medial Ganglionic Eminence-derived Interneurons) in which Rac1 is deleted. Notably, the deletion of the Rac1 protein is not fully achieved during developmental stages in MGE-derived interneurons, specifically in Parvalbumin-expressing Interneurons and Somatostatin-expressing interneurons. Approximately fifty percent of the Rac1fl/fl; Nkx2.1Tg(Cre); R26R-YFP+/– (referred to as Rac1 cKO) mice do not survive beyond three weeks after birth. The control group will consist of Rac1+/+; Nkx2.1Tg(Cre); R26R-YFP+/– mice, referred to as Rac1+/+; Nkx2.1+/Cre and Rac1 +/+;Nkx2.1+/+. On the other hand, the experimental group will include Rac1fl/fl; Nkx2.1Tg(Cre); R26R-YFP+/– animals, referred to as Rac1fl/fl; Nkx2.1+/Cre or Rac1 conditional knockout or Mutant.

Tag1

CNTN2/TAG-1, a member of the contactin subgroup within the immunoglobulin (Ig) gene superfamily, consists of six C2 class Ig-like domains and four fibronectin type III-like repeats in its ectodomain while being anchored to the plasma membrane by a glycosylphosphatidylinositol lipid domain. In a study [116] it was reported that a null mutation of CNTN2/TAG-1 was achieved through targeted mutation using homologous recombination. Specifically, a 5.2kb long DNA fragment spanning from exon II to exon IV was replaced with an 8kb long neomycin resistance gene (Neo) cassette, while diphtheria toxin (DT) was added for negative selection under the expression of MC1 receptor. The Neo and DT were inserted in reverse orientation to the CNTN2/TAG-1 gene. As a result, CNTN2/TAG-1 -/- mice lacking the CNTN2/TAG-1 protein, 130KDa, were generated and further studies showed that the mutant homozygous condition was not lethal based on observed ratios [116].

Regarding the morphology of CNTN2/TAG-1 mutant mice, investigations have demonstrated comparable size and structure of the central nervous system (CNS) between wild-type and knock-out mice at both postnatal day 2 (P2) and embryonic day 15 (E15) in regions such as the hippocampus, cerebellum, and spinal cord. In the cerebellum, where CNTN2/TAG-1 is typically co-expressed with calbindin, a specific marker for Purkinje cells, the mutant condition did not impact these cells [116]. Similarly, cortical plate neurons and cerebellar granule cells, which normally exhibit high CNTN2/TAG-1 expression, appeared unaffected by the absence of CNTN2/TAG-1. Although certain CNTN2/TAG-1 -/- mice exhibited spontaneous epileptic seizures, no overt phenotype was observed in the hippocampus of CNTN2/TAG-1 -/- mice [116]. From

DNA Extraction

DNA extraction from mouse tail tissue was performed using a well-optimized protocol to ensure reliable and efficient results. For each tail, a mixture of 50µl of 50mM NaOH and 50µl of 0.4mM EDTA was prepared. Following vortexing, 80-100µl of this NaOH-EDTA mix was added to individual tubes containing the mouse tail samples. Subsequently, the tubes were placed in a heat block set at 95°C for 1 hour, with regular vortexing every 20 minutes to promote thorough mixing and effective extraction. After the heat treatment, a final vortexing step was performed to ensure complete homogenization of the samples. To neutralize the reaction, an equal volume of neutralization buffer (40mM Tris, pH 8.0) was added, and another vortexing step was executed. The resulting DNA-extracted samples were then stored at -20°C, rendering them stable and suitable for future molecular analyses.

Mouse Genotyping for Rac1/Nkx2.1. And Tag1/DT-A Mouse lines

In order to identify the genomes of the mice, we performed a Polymerase chain reaction(PCR) for each of the mouse lines, Rac1 and Nkx2.1. The primers that were used can be seen in the table below.

Primers for Rac1,Nkx2.1, TAG1, And DT-A PCR reactions	
Primers for Rac1 PCR	
Rac1 b	5’- GAAGGAGAAGAAGCTGACTCCCATC-3’
Rac1 c	5’- CAGCCACAGGCAATGACAGATGTTC-3’
Primers for Nkx2.1. PCR	

Nkx2.1-iCre-Fw	5’- GTCCACCATGGTGCCCAAGAAGAAG-3’
Nkx2.1-iCre-Rev	5’- GCCTGAATTCTCAGTCCCCATCTTCGAGC-3’
Primers for TAG1 PCR	
TAG1.5’-2	GCTCTACAGCCCAGGCAGTTC
TAG1.3’	CTTTGCCACATTGTGCTGTG
Neo.3’	GAAGACAATAGCAGGCATGC
Primers for DT-A PCR	
Forward primer	5’-CCATGGATCCTGATGATGTTGTTG- 3’
Reverse primer	5’- GAATTCTCACAAAGATCGCCTGACACG -3’

Table 1: Primers for the RAC1, Nkx2.1, TAG1, and DT-A PCR reactions.

The following tables show the concentration and the volume of all the media for all the PCRs and the temperatures and time periods for all the steps of the PCRs.

Table 2: The concentration and volumes of all the media for the RAC1 and Nkx.2.1 PCRs

RAC 1			Nkx2.1		
Media	Concentration	Volume	Media	Concentration	Volume
Genomic DNA	-	2 µl	Genomic DNA	-	2 µl
Buffer (Enzyquest)	1x	2 µl	Buffer (Enzyquest)	1x	2 µl
dNTPs	2 mM	2 µl	dNTPs	2 mM	2 µl
Rac1 b primer	10 mM/µl	1 µl	Rac1 b primer	10 mM/µl	1 µl
Rac1 c primer	10 mM/µl	1 µl	Rac1 c primer	10 mM/µl	1 µl

Taq Polymerase	2.5 units/µl	0.6 µl	Taq Polymerase	2.5 units/µl	0.5 µl
ddH2O	-	11.4 µl	ddH2O	-	11.5 µl

Table 3: The concentration and volumes of all the media for the TAG1 and DT-A PCRs

TAG 1			DT-A		
Media	Concentration	Volume	Media	Concentration	Volume
Genomic DNA	-	2 µl	Genomic DNA	-	2 µl
Buffer (Enzyquest)	1x	2 µl	Buffer (Enzyquest)	1x	2 µl
dNTPs	2 mM	2 µl	dNTPs	2 mM	2 µl
TAG1.5'-2	10 pmol/µl	1 µl	Forward primer	100 ng/µl	0.2 µl
TAG1.3'	10 pmol/µl		Reverse primer	100 ng/µl	0.2
Neo.3'	10 pmol/µl	1 µl	Taq Polymerase	2.5 units/µl	0.4 µl
Taq Polymerase	2.5 units/µl	0.7 µl	ddH2O	-	13.6 µl
ddH2O	-	10.3 µl	-	-	-

Table 4: The PCR's conditions for the Rac1, Nkx.2.1, TAG1, and DT-A PCRs. The temperature is referred to as "Temp" inside the table to save space.

Rac 1			Nkx2.1		TAG1		DT-A	
PCR steps	Temp	Time	Temp	Time	Temp	Time	Temp	Time
Denaturation	94oC	3'	94oC	5'	95oC	3'	95oC	3'
Denaturation	94oC	30''	94oC	1''	95oC	30''	95oC	30''
Annealing	60oC	30''	63oC	1''	60oC	30''	60oC	30''
Extension	72oC	30''	72oC	1''	72oC	1'	72oC	1''
Final Extension	72oC	3'	72oC	10'	72oC	5'	72oC	5'

Hold	4oC	∞	4oC	∞	4oC	∞	4oC	∞

Mowiol Mounting Medium Preparation

The Mowiol mounting medium was meticulously prepared by combining specific reagents in precise proportions. Firstly, 2.6g of Mowiol 4-88 (Fluka, #81381, Sigma) was added to 6g of glycerol, and the mixture was stirred to ensure thorough mixing. Subsequently, 6mL of H2O was added to the mixture, and the solution was allowed to stand at room temperature for several hours. To this, 12mL of 0.2M Tris-Cl (pH 8.5) was added, and the resulting solution was heated to 50°C for 10 minutes, with periodic mixing. Upon complete dissolution of Mowiol, the solution was clarified through centrifugation at 5000 g for 15 minutes. The prepared Mowiol mounting medium was then aliquoted into tubes and stored at −20°C.

Long-Term Dissociated Primary Cortical Neuronal Cultures

Mouse mixed cortical cultures were derived from embryos at gestational day E16.5, with embryonic day E0.5 being the reference point for the detection of the copulation plug, signifying the beginning of pregnancy. The cells were cultured for a total of 16 days, allowing for their maturation and development, before proceeding with fixation and subsequent immunocytochemistry analyses.

Coverslip Preparation

18 mm coverslips (for 12-well plates) or 12 mm coverslips (for 24-well plates) were immersed in a container filled with 68% nitric acid (HNO3) for an overnight incubation period. This step allowed for effective cleaning and surface preparation. After the overnight incubation, the coverslips were removed from the HNO3 bath and subjected to thorough rinsing with deionized distilled water (ddH2O). Rinsing was performed using a rocker to ensure even coverage and complete removal of any residual acid. The coverslips underwent four rinses, each lasting approximately one hour. Subsequently, the coverslips were transferred to a container with 100% ethanol (Et-OH) for a 1-hour rinse on the rocker. This step further eliminated any remaining impurities from the coverslip surfaces, promoting enhanced adhesion of biological specimens during subsequent experiments. Following the ethanol rinse, the coverslips were carefully spread on a paper surface under the protection of a hood. The coverslips were then exposed to ultraviolet (UV) light for approximately 15 to 20 minutes to facilitate drying and sterilization, creating a clean working surface. Upon thorough drying, the prepared coverslips were stored inside sealed Falcon tubes or petri dishes, both securely

placed inside the hood. This storage method ensured the coverslips remained uncontaminated and ready for future experiments.

PDL Coating

To initiate the coverslip preparation, five aliquots of poly-D-lysine (PDL) stocks (1mg/ml) were thawed. Under sterile conditions within the hood, individual CoverSlips were placed in each well of a culture plate and subjected to a single rinse with sterile deionized distilled water (ddH2O) at a volume of 1ml per well. Subsequently, the CoverSlips were coated with PDL, which was appropriately diluted to a final concentration of 0.2mg/ml in sterile ddH2O at a volume of approximately 0.7ml per well. The PDL-coated CoverSlips were then incubated overnight at 37°C within an incubator, promoting optimal coating adherence and preparatory stability for subsequent experimental procedures. The following day, the PDL was carefully removed from each well using an aspirator, and the coverslips were rinsed meticulously with sterile ddH2O for a total of four times. After the final wash, excess ddH2O was removed, and the coverslips were allowed to dry completely under the hood. In cases where a PDL-coated well plate is not utilized in an experiment, it can be stored at 4°C for 1-2 weeks with ddH2O present in each well, ensuring its preservation for future use.

Cortex dissection and Cultures Plating

Pregnant E16.5 female mice were euthanized by cervical dislocation. The placenta with the embryos was carefully dissected and placed in a petri dish containing an ice-cold Dissecting Buffer (DB) composed of 1x sterile phosphate-buffered saline (PBS) or 1x HBSS. The embryo brains were then dissected, 2-4 brains at a time, under a stereoscope. The meninges were removed, and the cortices were collected in ice-cold DB. Subsequently, 2-4 cortical chunks were placed in 1.5 ml sterile Eppendorf tubes with 1 ml of ice-cold DB and 10 µl 0.2 mg/ml DNAse, where each embryo contributed to 1 cortex or 2 cortex chunks.

The collected chunks were gently washed twice with ice-cold DB (1 ml per tube) using a pipette. After removing the liquid, the chunks were replaced with 900 µl of DB and 100 µl of 10x Trypsin 2.5% with 10 µl of DNAse 0.2mg/ml, initiating the trypsinization procedure for chemical dissociation. The tubes were gently inverted to mix the chunks, and incubation was carried out at 37°C in a heat bath (inside the incubator) for 10-15 minutes until the chunks broke down. During this time, the mixture was occasionally mixed by gently inverting the tubes every 3-5 minutes. Following incubation, the chunks were allowed to settle, and then washed three times with ice-cold DMEM with FBS (See table below)(1 ml per tube) to remove and inactivate trypsin, with careful removal of the liquid after each wash. For the 3rd wash, 1 ml of ice-cold DB and 10 µl of DNAse (0.2 mg/ml final concentration) were added. The cells were mechanically dissociated through gentle up-and-down pipetting using a p1000 blue tip (at 850 µl) for a maximum of 10 times and 5 times with a p200 yellow tip to achieve the trituration procedure.

The procedure was carried out carefully to avoid bubbles, harsh pipetting, and excessive up-and-down motions (no more than 15 times), which could lead to significant cell death and jeopardize cell culture health. The cells were then centrifuged at 500g for 5 minutes at 4°C to pellet down the cells.

The supernatant was carefully removed, and the cell pellet was resuspended in fresh ice-cold Plating Medium with 4-5 pipetting using a 1000p tip. To remove any large residual chunks, the cells can be passed through a pre-wetted 70 µm size cell strainer with Plating Medium dilution (1:5-1:10) (See table below) within a 50 ml Falcon tube to aid cell counting, which is optional, as it may increase stress. Using a Hoezbauer Cell counter, 10 µl of the cell mix was taken to count the cells in 2 diagonal squares of the 12 x squares. The total number of cells in the final volume of the mix was calculated, and 200,000 to 500,000 cells were plated in each well, maintaining a medium density. Each well was supplied with approximately 1 ml of fresh Plating Medium, and the cells were agitated slowly to evenly distribute them on the coverslip.

The plated cells were incubated at 37°C in a cell-culture CO2 incubator for 16 days. On the 3rd day of incubation, half of the medium was removed from the cells, and the same amount of fresh warm 37°C Feeding Medium (See table below) with 2x AraC 1:1000 was added. The AraC was changed the next day and left overnight. The cells were then fed every 3rd day (Dev 6-9-12, etc.) by removing 300-500 µl of the old medium and replacing it with the same amount of fresh warm Feeding Medium, with additional medium added if evaporation occurred.

Table 5: Mediums for the Long-Term Primary cortical Cultures

Plating Medium	For **50** ml	**Feeding Medium**	For **50** ml	**FBS with DMED**	For **10** ml
Neurobasal plus medium	48 ml	Neurobasal plus medium	48.5 ml	FBS	3 ml
B27 (50x)	1 ml	B27 (50x)	1 ml	DMEM	7 ml
1%v/v FBS	0.5 ml	Pen/Strep(PSG) 100x	0.5		
Pen/Strep(PSG) 100x	0.5 ml				

B27: gibco/ThermiFisher(Ref: 17504-044)

Neurobasal Plus Medium: gibco/Thermifisherm (Ref: A3582901)

Cell Fixation

After the designated incubation period, half of the medium in each well was gently removed, and an equal volume of 8% paraformaldehyde (PFA) was added to each well. The cells were then incubated with the PFA solution for 15 minutes at room temperature (RT) to initiate post-fixation. Following the post-fixation step, the medium with PFA was slowly and carefully removed to avoid any disruption to the cells. The wells were subjected to three consecutive washes with 1x phosphate-buffered saline (PBS) in a gentle manner to ensure minimal impact on the cells. These PBS washes effectively removed any remaining PFA while preserving the integrity of the cultured neurons. Finally, they were stored at 4oC to be later used for immunocytochemistry.

Immunocytochemistry of cell cultures

For the initial blocking step, a blocking solution consisting of 1% bovine serum albumin (BSA) and 0.1% Triton X-100 in 1x phosphate-buffered saline (PBS) was prepared. Approximately 30 µl of the blocking solution was placed on a parafilm. Using a curved needle and curved point forceps, each coverslip (CS) containing the cells was carefully lifted from the well and transferred to the drop of blocking solution. The coverslips were then incubated at RT for 30 minutes to allow for effective blocking of non-specific binding sites. Following the blocking step, fresh drops of primary antibodies (~30 µl) were placed on a new parafilm. Subsequently, the coverslips were gently repositioned on top of the drops containing the primary antibodies. Incubation at RT was carried out for 1-1.5 hours, considering the optimal time required for efficient antibody binding depending on the antibody's effectiveness.

To remove unbound primary antibodies and minimize non-specific binding, three consecutive washes in 1x PBS were performed. A petri dish with parafilm was utilized to facilitate the washing process. The coverslips were placed with the cells facing upwards, and a transfer pipette was carefully used to apply 1x PBS along the side of each coverslip and then gently remove any excess liquid using a 1000 pipette. This wash step was repeated thrice to ensure thorough and effective removal of unbound antibodies.

For the secondary antibody incubation, fresh drops of secondary antibodies (~30 µl) were placed on a new parafilm, and each coverslip was cautiously transferred to the respective drop of secondary antibodies. The incubation was carried out at RT in a dark environment to prevent light-induced bleaching and maintain the integrity of the fluorophores. Dapi staining was prepared at a dilution of 1:1500 in 1x PBS. A drop of Dapi staining solution was placed on a new parafilm, and each coverslip was positioned on the drop. The coverslips were allowed to incubate in the dark at RT for 5 minutes to enable specific nuclear staining.

Following Dapi staining, three additional washes in 1x PBS were conducted to eliminate any residual staining solution. Similar to the previous wash steps, the coverslips were carefully placed with the cells facing upwards, and 1x PBS was applied along the side of each coverslip using a transfer pipette. The process was repeated three times to ensure thorough removal of excess staining solution.

Finally, a small drop of Mowiol was carefully positioned on the slide, ensuring minimal contact with the CS using the yellow tip of the pipette. Subsequently, with the aid of forceps, the CS was slowly and gently placed at an angle on the slide, facilitating the even spreading of Mowiol across the entire CS surface. To protect the mounted tissue and prevent any damage during storage, nail polish was applied the following day to securely seal the coverslip. This isolation step provided a safeguard against potential disruption or contamination. The immunostained and mounted CS was then stored at 4°C, maintaining its integrity and preserving the fluorescent signal for subsequent examination and analysis.

Table 6: Antibodies used for ICC are described in the following table.

Primary Antibodies					**Secondary Antibodies**		**Nuclear Staining**	
Antibody	**Host**	**Company**	**Catalog number**	**App (ICC)**	**Antibody**	**App**	**Antibody**	**App**
Somatostatin (SST)	mouse	Santa Cruz Bio.	PVG-213	1/500	a-ms Alexa 555	1/800	Hoechst	1/2000
Gephyrin	rabbit	Synaptic Systems	147 003 or 147018	1/500	A-rb Cy2	1/800	Hoechst	1/2000
VGAT	G.pig	Synaptic Systems	131004	1/500	a-rb Alexa 647	1/800	Hoechst	1/2000
Synapsin-1	G. pig	Synaptic Systems	106104	1/1000	a-ms Alexa 647	1/800	Hoechst	1/2000
PSD-95	rabbit	Synaptic Systems	124003	1/500	A-rb Cy2	1/800	Hoechst	1/2000

Confocal Imaging and Analysis

Confocal Imaging

Confocal microscopy images were obtained using a Leica TCS-SP8 confocal laser scanning microscope (Leica Microsystems) (a 40× objective, 1.4 NA oil objective). Pixel Size was set on 0,284 µm. Up to 22 images with a Z-interval of 0.5 um were acquired per stack. Zoomed-in insets were generated via Quick Figures in FIJI open software.

Synaptic puncta quantification

Co-localization puncta of pre- and post-synaptic puncta on labeled SST+ INs was used to identify the structurally accomplished synapses on SST INs, which were termed completed synapses. VGAT and Gephyrin were assumed to be presynaptic and postsynaptic markers, respectively, for inhibitory synapses. Synapsin-1 and PSD-95 were assumed to be presynaptic and postsynaptic markers, respectively, for excitatory synapses. Quantification of overlapping co-localization puncta on SST+ stained cells was performed manually. 49 primary SST+ neurons from 2 animals and 45 cells from 2 Rac1cKO animals were used for the co-clustering puncta analysis. We measured perisomatic inhibitory synapse density at least 21 slices separated by 0,5 um intervals, that constitute a 10 um z-stack.

Perisomatic synapse densities were calculated by dividing the total number of perisomatic synapses by soma perimeter (in um). Synapse densities on the primary dendrites were calculated by dividing the total number of synapses across the length of dendrites coming from the SST CINs. We classified non-somatic synapses as proximal based on their location on the dendrites of the postsynaptic cell. All synapses that were formed within 20 um from soma and onto a 1st-order dendritic branch were considered proximal.

Imaging and synapse density quantification were based on certain limitations, such as Gephyrin cluster size, which has been previously reported to range from 100-300 nm, and PSD95 cluster size ranging from 90-298 nm [117]. Moreover, synapses are miniature structures, with a typical size range of 200–500 nm in diameter [70,118], according to electron microscopy data.

Statistical analysis

All data were analyzed with Fiji/ImageJ and statistical analysis was performed using Python version 3. Data are expressed as mean ± standard deviation of the mean (SEM). The statistical significance of differences ($p < 0.05$) was measured using a two-tailed, unpaired nonparametric Student's t-test.

Electrophysiological Recording

Electrophysiological recordings were conducted in Professor Sidiropouolou's laboratory at the Biology Department of the University of Crete, with the assistance of Lida Vagiaki. The experimental procedure involved the decapitation of mice after cervical dislocation, followed by immediate removal of the brain and placement in ice-cold, oxygenated artificial cerebrospinal fluid (aCSF). Brain slices, approximately 400 μm thick, containing the hippocampus were obtained using a vibratome. The slices were then allowed to equilibrate in a submerged chamber with oxygenated (95% O2/5% CO2) aCSF containing (mM): 125 NaCl, 3.5 KCl, 26 NaHCO3, 2 CaCl2, 1 MgCl2, and 10 glucose (pH 7.4, 315 mOsm/L) for at least an hour before the experiments commenced. Subsequently, the slices were transferred to a submerged recording chamber continuously superfused with oxygenated aCSF at room temperature.

The extracellular recording electrode, filled with NaCl (2M), was positioned within the upper layers of the PFC or barrel cortex (BC). Additionally, a platinum/iridium metal microelectrode was placed in the upper layers of the PFC or the stratum radiatum layer of the CA1 region of the hippocampus, approximately 300 μm away from the recording electrode. This microelectrode was used to evoke field excitatory postsynaptic potentials (fEPSPs). The recorded responses were amplified using a Dagan BVC-700A amplifier and digitized using the ITC-18 board on a PC, with custom-made procedures in IgorPro software. Data acquisition and analysis were carried out using custom-written procedures in IgorPro software.

For the long-term potentiation (LTP) experiments in the hippocampus, baseline responses were recorded for at least 20 minutes. Subsequently, theta-burst stimulation was applied, involving five pulses at 100 Hz, repeated four times at the theta-rhythm (every 200 ms). After the theta-burst stimulation (Time=0), the recording continued with a pulse of 100 pA administered every 1 minute for 50 minutes. The experiment was performed in 2 WT mice (DT-A -, TAG1 +/+), which were used as control, and 3 KO mice (DT-A -, TAG1 -/-)

Analysis Of The Electrophysiological Recording

In our LTP analysis, we assessed the percentage of field EPSPs (fEPSPs) by comparing the responses in control and KO mice. This percentage was computed at each time point by taking the average values from both groups. Specifically, we concentrated on the difference between the minimum EPSP value and the baseline current response before the current administration. This difference was then divided by the same average derived from the baseline current response recorded before theta-burst stimulation (Time=0). The analysis was conducted with assistance from Professor Sidiropoulou’s lab.

Results

To investigate the impact of Rac1 on the development of a specific subset of cortical interneurons originating in the MGE, we utilized a mouse model in which Rac1 was selectively deleted from MGE-derived inhibitory neurons, specifically PV and SST CINs. This manipulation was achieved by combining a floxed allele of Rac1 (Rac1fl) [113] with the Nkx2.1-Cre transgene [93114], which serves to mark PV and SST CINs [5,49,114]. The expression of Nkx2.1, a critical transcription factor governing the development of MGE-derived CINs, commences at embryonic day 9 (E9) [49], signifying the initiation of Rac1 elimination from MGE-derived cells by E12 [58]. The introduction of the Rosa26StopYFP reporter further facilitated the visualization and tracking of cortical PV and SST cells expressing Cre [115].

Prior investigations conducted within our research group had unveiled several notable deficiencies in Rac1 conditional knockout (Rac1cKO) mice. Most notably, there was a 50% reduction in the population of MGE-derived cells reaching the cortex [58], which, in turn, resulted in impaired synaptic plasticity in the adult prefrontal cortex (PFC) [95]. Additionally, these mice exhibited increased synaptic transmission, disrupted oscillatory brain activity, and an overall shift toward hyperexcitation in the adult barrel cortex [96].

However, our current understanding of the specific role of Rac1 in the maturation of individual CINs during early postnatal stages is limited. Building upon our previous findings, we formulated a hypothesis that Rac1 may exert influences on the morphological characteristics and synaptogenesis of CINs during these critical developmental phases, potentially in a cell-type-specific manner. As part of our investigation, we analyzed the soma size of SST CINs, followed by a meticulous quantification of synapse density on these specific interneurons.

Increased soma size of the Rac1-deficient SST CINs in vitro

In the context of SST-expressing CINs, as determined through SST staining, our analysis focused on the measurement of soma perimeter in labeled CINs, encompassing both control and Rac1 mutant mice. The dataset comprised two animals per group, and an approximate count of 20 SST+ cells was performed for each animal. Our measurements unveiled a statistically significant increase in the soma perimeter of SST-expressing cells as a consequence of the conditional ablation of Rac1 from MGE-derived INs when compared to their control littermates. This notable difference in soma perimeter is visually evident in representative images from both experimental groups, as illustrated in Figure 6

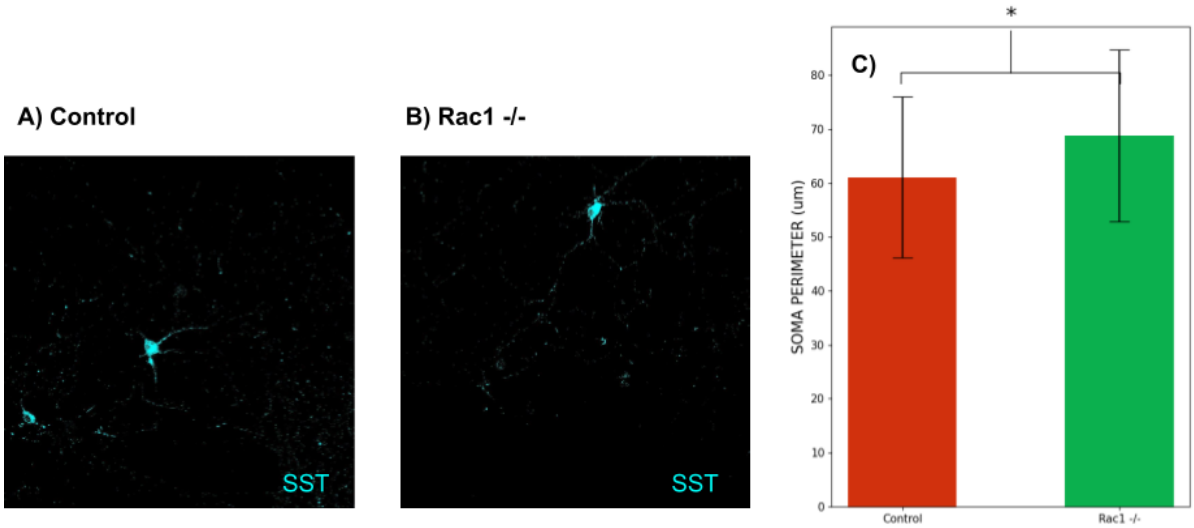

Figure 6: Ablation of Rac 1 specifically from MGE-derived cells results in increased soma perimeter in SST+ CINs. A+B) Representative confocal images of immunocytochemical labeling for SST(cyan) in primary cortical interneurons, prepared from control (A) and Rac1 cKO (B) mice. Cells were dissociated from embryos at day E16,5 and stained 16 days after plating (DIV1). C) Statistical significance of an increase in soma perimeter of Rac1cKO mice compared to control. Data are expressed as mean ± standard deviation of mean (SEM). Statistical significance ($P<0.05$) of change in soma perimeter was measured using an unpaired t-test. In total, 46 cells from n=2 control mice and 45 cells from n=2 Rac1cKO mice were used for this type of analysis.

Rac1 Ablation results in decreased levels of excitatory synapses on the soma and primary dendrites of SST CINs

After observing differences in soma characteristics between the two groups, we sought to investigate whether there were distinctions in synaptic density as well. To address this, we utilized cells obtained from mixed cortical cultures derived from both control (Figure 7) and Rac1cKO mice (Figure 8), which had been maintained in culture for 16 days. These cells were subjected to staining against SST, Hoechst as a nuclear marker, and excitatory synaptic markers. Our study focused on two prominent excitatory synaptic proteins: Synapsin-1 and PSD-95. Synapsin-1 functions as an excitatory presynaptic marker, primarily located in vesicles containing glutamate neurotransmitters. In contrast, PSD-95 is a scaffold protein found in the postsynaptic neuron, responsible, among other roles, for the proper localization of receptor proteins. Significantly, excitatory synapse density on the primary dendrites of SST+ CINs from Rac1cKO mice was observed to be notably reduced compared to that of SST+ cells from control mice (as depicted in Figure 9A).

Furthermore, we conducted an assessment of the co-localization of synaptic markers on the primary dendrites of SST+ CINs. To provide a more specific quantification, we counted the puncta and divided them by the length of the dendrites on each SST+ interneuron. As demonstrated in Figure 9B, in alignment with the soma findings, excitatory synapse levels exhibited a decrease in the Rac1cKO group when compared to the control group.

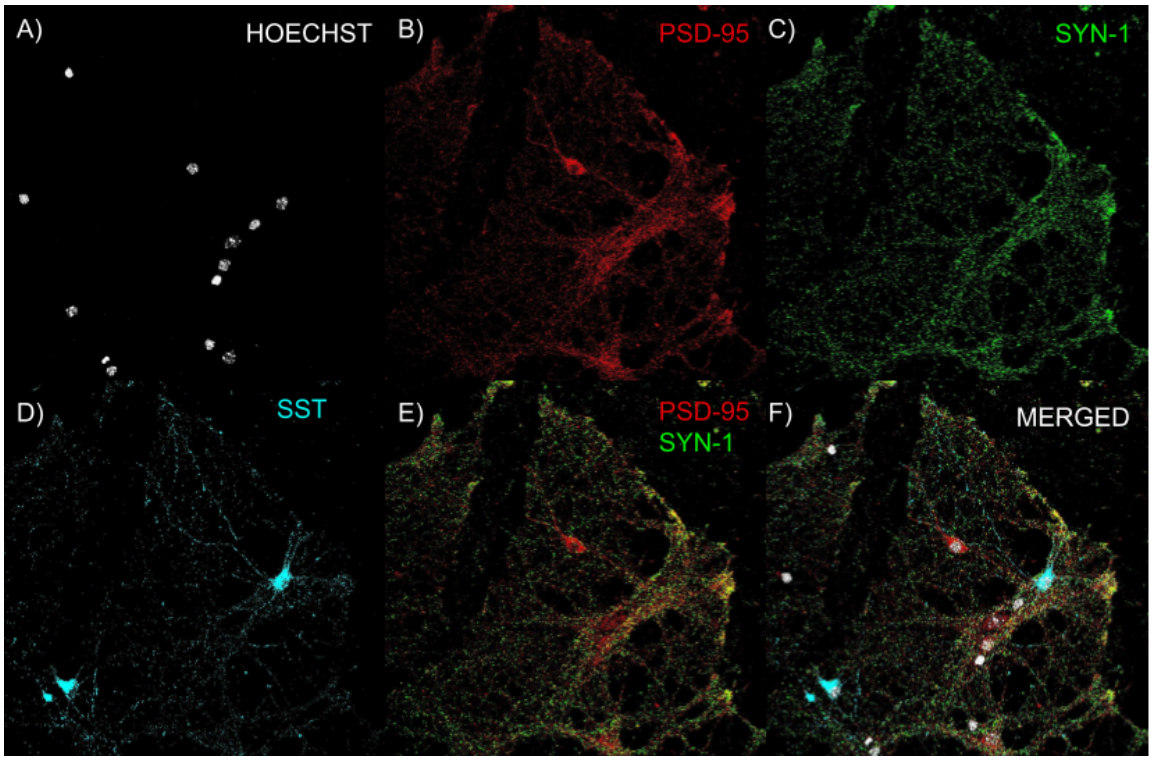

Figure 7: Representative images of immunocytochemical in primary CINs, isolated from control WT mice labeling for A) Hoechst (Gray), B) PSD-95 (red), C) Synapsin-1 (green), D) SST (cyan), E) Merge of PSD-95 and Synapsin-1. Overlay of PSD-95/Synapsin 1 colocalization puncta, represents the number of excitatory synapses. , and F) merge picture of all the previous markers. Cells were previously isolated from E16.5 control and kept in culture for 16 days.

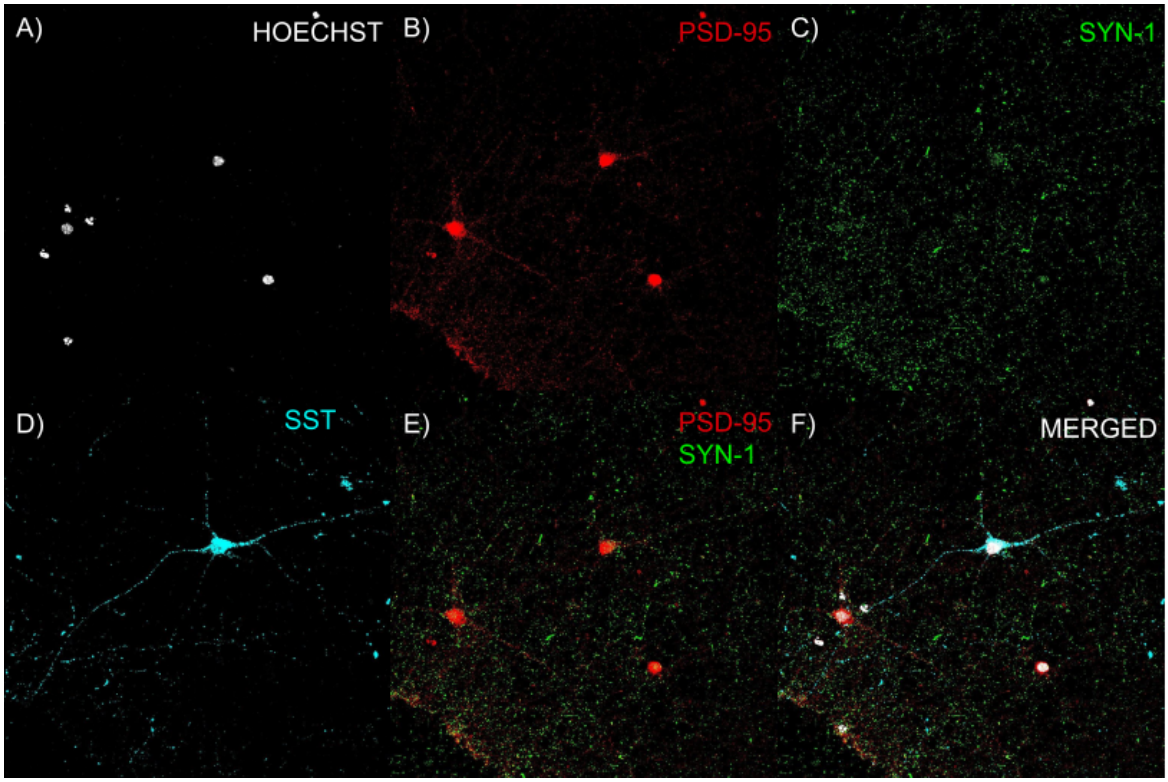

Figure 8: Representative images of immunocytochemical in primary CINs, isolated from Rac1cKO mice labeling for A) Hoechst (Gray), B) PSD-95 (red), C) Synapsin-1 (green), D) SST (cyan), E) Merge of PSD-95 and Synapsin-1. Overlay of PSD-95/Synapsin 1 colocalization puncta, represents the number of excitatory synapses. , and F) merge picture of all the previous markers. Cells were previously isolated from E16.5 Rac1cKO mice and kept in culture for 16 days.

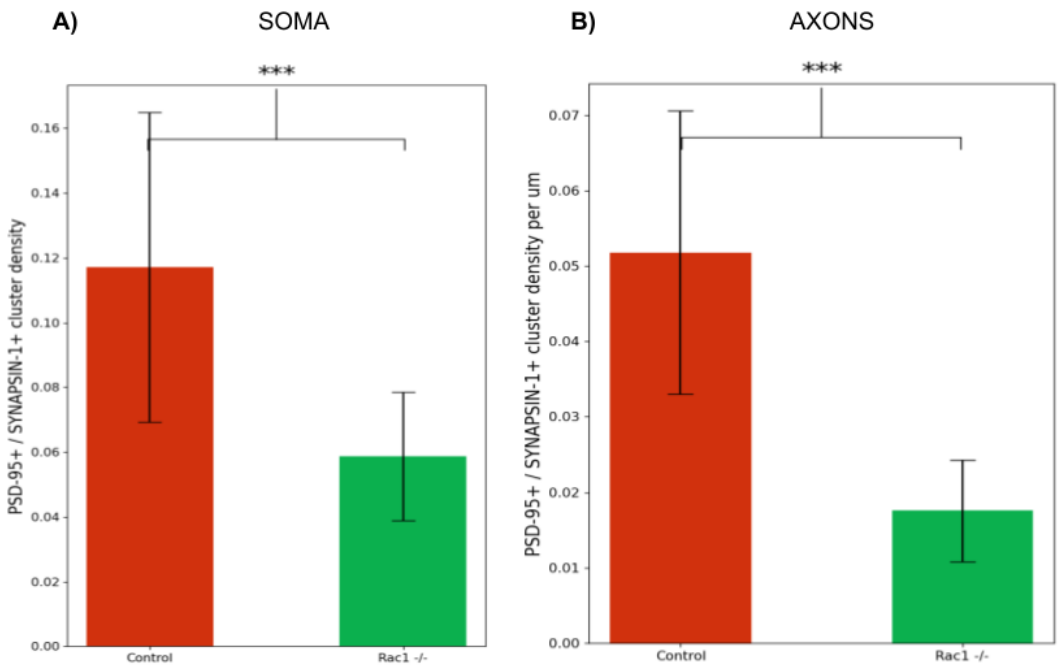

Figure 9: Significantly fewer excitatory synapses were formed on the soma (A) and the primary dendrites (B) of SST+ CINs from Rac1cKO mice compared to the control group. Data are expressed as mean ± standard deviation of the mean (SEM) (puncta/ soma's diameter in um and puncta/dendrites' length in um). Statistical significance (P<0.001) of change in synapse density was measured using an unpaired t-test. In total, 25 cells from n=2 control mice and 23 cells from n=2 Rac1cKO mice were used for this type of analysis.

Rac1 Ablation results in a decreased number of inhibitory synapses on the soma and primarily dendrites of SST CINs

To investigate the impact of Rac1 GTPase depletion on synapse formation during the maturation of SST-positive cells, we conducted immunocytochemistry, labeling primary cells with the nuclear marker Hoechst, SST, and concomitantly using antibodies against synaptic markers, specifically vesicular GABA transporter (VGAT) and Gephyrin (Figures 9 and 10). VGAT serves as an inhibitory presynaptic marker, predominantly localizing to synaptic vesicles in GABAergic neurons, while Gephyrin functions as an inhibitory postsynaptic marker, acting as a scaffold protein within the postsynaptic neuron.

Initially, we quantified inhibitory synapse density on the soma of SST+ CINs by assessing the co-localization of puncta formed by pre- and postsynaptic markers overlapping with labeled SST+ CINs (Figure 11A). Intriguingly, inhibitory synapses on the soma of PV+ INs derived from Rac1 cKO mice were found to be significantly fewer compared to those on SST+ INs from control mice, as shown in Figure 14.

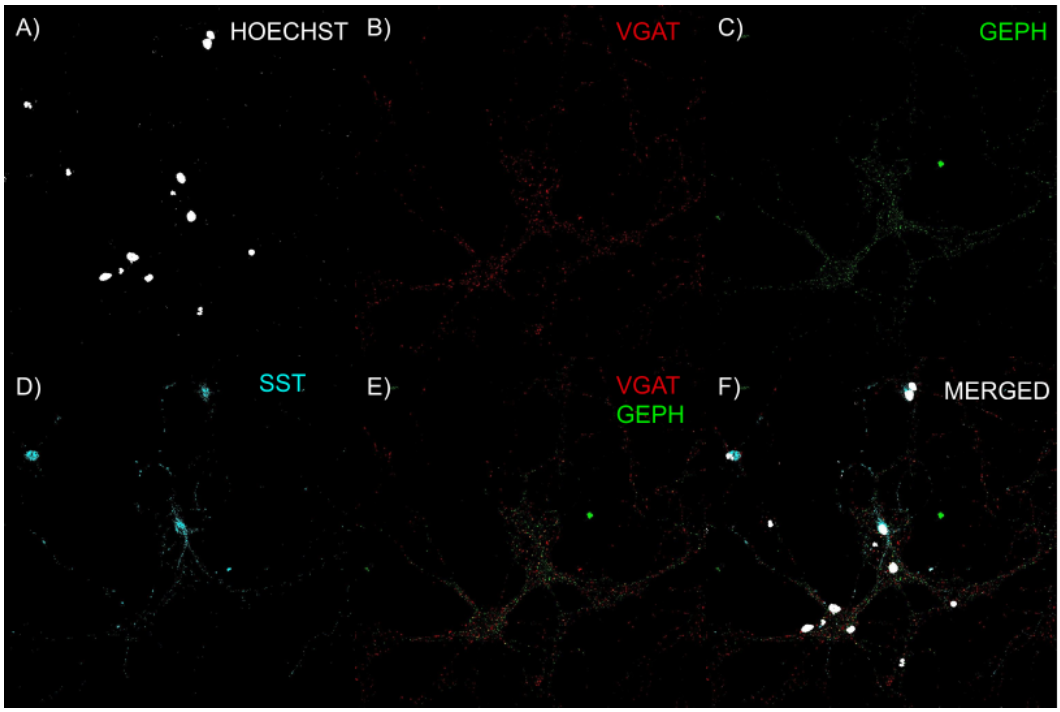

Figure 9: Representative images of immunocytochemical in primary CINs, isolated from control WT mice labeling for A) Hoechst (Gray), B) V-GAT (red), C) Gephyrin (green), D) SST (cyan), E) Merge of V-GAT and Gephyrin. The overlay of V-GAT/Gephyrin co-localization puncta represents the number of inhibitory synapses and F) merged picture of all the previous markers. Cells were previously isolated from E16.5 control and kept in culture for 16 days.

Additionally, in order to quantify proximal inhibitory synapses formed on the primary dendrites of SST+ CINs in both groups, VGAT and Gephyrin co-localization were assessed in a similar manner (as indicated in Figures 9 and 10). The analysis revealed a significant reduction in the number of inhibitory synapses on the primary dendrites of SST+ CINs with Rac1 deletion (Figure 11B).

In summary, our findings suggest that the early developmental ablation of Rac1 from MGE-derived CINs leads to altered synapse density on SST-expressing CINs during the early postnatal stages. Specifically, both excitatory, as evidenced by Synapsin-1/PSD-95 colocalization quantification, and inhibitory synapses, as indicated by VGAT/Gephyrin colocalization, were significantly reduced on both the soma and primary dendrites of Rac1 mutant SST+ CINs in vitro.

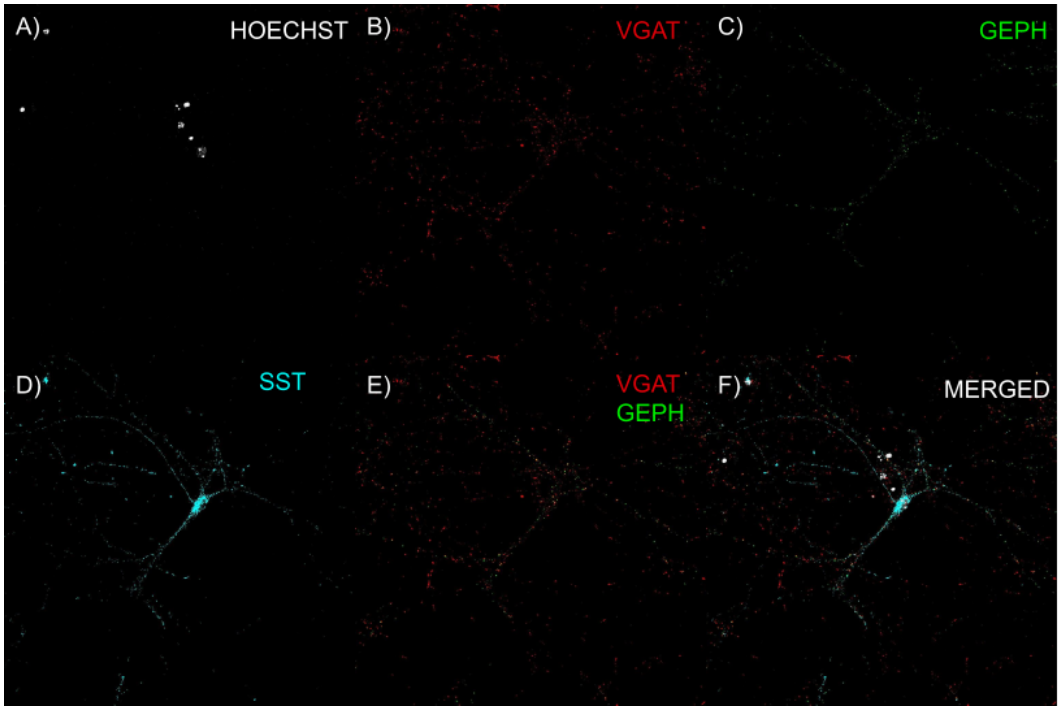

Figure 10: Representative images of immunocytochemical in primary CINs, isolated from Rac1cKO mice labeling for A) Hoechst (Gray), B) V-GAT (red), C) Gephyrin (green), D) SST (cyan), E) Merge of V-GAT and Gephyrin. The overlay of V-GAT/Gephyrin co-localization puncta represents the number of inhibitory synapses. , and F) merge picture of all the previous markers. Cells were previously isolated from E16.5 Rac1cKO and kept in culture for 16 days.

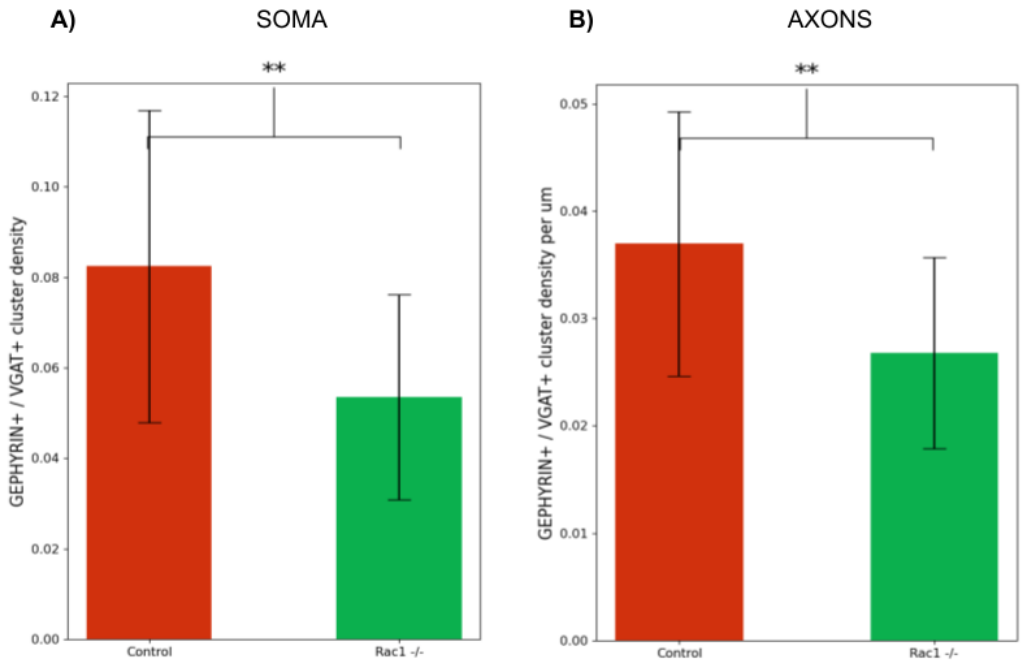

Figure 11: Significantly fewer inhibitory synapses were formed on the soma (A) and the primary dendrites (B) of SST+ CINs from Rac1cKO mice compared to the control group. Data are expressed as mean ± standard deviation of the mean (SEM) (puncta/ soma's diameter in um and puncta/dendrites' length in um). Statistical significance (P<0.001) of change in synapse density was measured using an unpaired t-test. In total, 23 cells from n=2 control mice and 24 cells from n=2 Rac1cKO mice were used for this type of analysis.

LTP Recordings In The CA1 Area Of The Hippocampus

In the next experiment CNTN2/TAG-1 KO (DT-A -; TAG1 -/-) and WT (DT-A -; TAG1 +/+) mice were used to examine the induction and maintenance of LTP in the hippocampal CA1 area. As shown in Figure 8, after the theta-burst stimulation the KO animals had decreased LTP response almost identical to the baseline recordings, which were recorded before the theta-burst stimulation. On the other hand, the WT mice had increased response, as expected where we can see the increase in the percentage of fEPSPs peak and the traces above. This behavior may be a result of two possible reasons. First, it may occur due to an increase in the excitation of the SST interneurons in the CNTN2/TAG-1 KO animals, which increases the inhibition of the pyramidal neurons, which are the target of the SST interneurons. The other possible reason is that there is a difference in NMDA receptors between the CNTN2/TAG-1 WT and KO animals, which results in the decrease of the LTP response after the theta-burst stimulation.

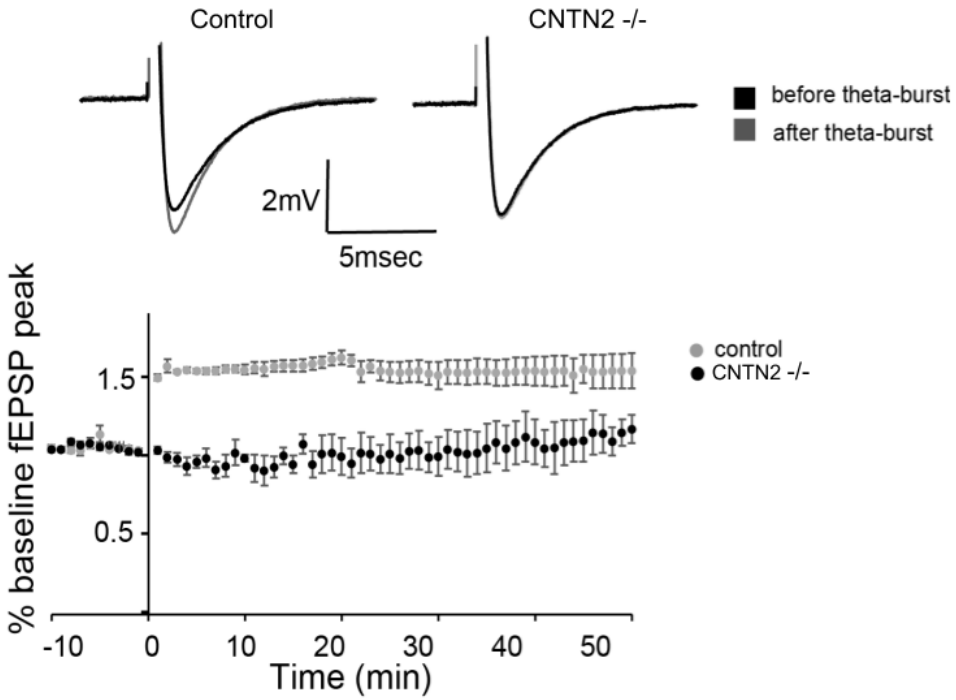

Figure 11: Graph showing the potentiation of the fEPSP following theta-burst stimulation in the CA1 area of the hippocampus in CNTN2/TAG1 KO(n=3) and WT animals(n=2). There is a statistically significant difference between the two groups (Two way repeated measures ANOVA; $F(1.52)=19.3$, $p=0.0005$) with every time point to be statistically significantly different (Post-hoc Tukey test for 5-time points; 10 seconds: $p=0.000006$, 20 seconds: $p=0.001$, 13 seconds: $p=0.0001$, 40 seconds: $p=0.00004$, and 50 seconds: $p=0.04$). This may result from either an increase in the excitation of the SST interneurons or a difference in the NMDA receptors between the 2 groups.

Discussion

Despite constituting a relatively small fraction of cortical neurons, GABAergic CINs have emerged as significant contributors to cortical function and are implicated in various neurological disorders, including schizophrenia, epilepsy, and autism spectrum disorders. These cells exhibit substantial diversity in terms of morphology, molecular profiles, and functions, a diversity shaped by genetic programs and activity-dependent mechanisms during their development.

Progress has been made in identifying molecules that govern CIN development, yet a more comprehensive understanding of intracellular molecules and their precise roles in CIN development is essential. Among these molecules, the small GTPase Rac1 has garnered attention due to its purported pivotal role in various stages of CIN development. Rac1 deficiency results in a 50% reduction in the number of IN-progenitors reaching the cortex, leading to impaired plasticity, heightened synaptic transmission, and disrupted oscillatory activity. However, the specific role of Rac1 in CIN maturation remains elusive.

Hence, this study aimed to investigate the influence of Rac1 on the morphological development and synaptogenesis of CINs during the early postnatal period. Given the substantial distinctions among various CIN types and prior evidence highlighting cell type-specific actions of Rac1, our study specifically focused on SST-expressing CINs.

Aberrant Morphology of Rac1-deficient SST CINs

Our objective was to investigate whether the absence of Rac1 from MGE-derived INs, specifically PV and SST CINs, impacts their morphological development during the early postnatal period. To address this inquiry, we utilized primary mixed cortical cultures obtained from control and IN-specific Rac1 cKO mice at E16.5. These primary cultures were nurtured for 16 days, with the day of plating designated as DIV1.

Our immunocytochemical examinations disclosed a noteworthy increase in the soma perimeter of SST CINs that successfully populated the mature cortex in the absence of Rac1. Interestingly, earlier investigations employing immunohistochemistry on E13.5 brain sections had not revealed any morphological disparities (e.g., length and branching) between control and

mutant interneurons once they had migrated away from the MGE and approached the pallial-subpallial boundary [58]. However, Rac1-deficient cells that failed to migrate towards the cortex, remaining aggregated in the ventral telencephalon when cultured in vitro, exhibited discernible morphological defects. These included issues about the actin cytoskeleton within their growth cones, as well as affected growth cones themselves and notably shorter neurites. These findings align with the previously reported roles of Rac1 in orchestrating cytoskeletal dynamics [53,54,59].

Studies investigating Rac1's morphological development in various neuronal populations have revealed differential roles, potentially modulated by distinct developmental timeframes. For instance, silencing Rac1 using siRNA in primary hippocampal neurons resulted in a marked reduction in dendritic length compared to luciferase-treated controls [60]. Conversely, overexpressing Rac1 in primary hippocampal neurons increased dendritic spine density, and re-expressing Rac1 in Rac1/3 double-knockout neurons restored spinogenesis [69].

It is worth noting that the deletion of Rac1 influences cell morphology which is not surprising, given its role as a Rho GTPase in the assembly and reorganization of actin and microtubule cytoskeletons. Microtubules and actin filaments represent foundational constituents of the cytoskeleton and are integral for defining cellular morphology [119,120].

Decreased excitatory and inhibitory synapse density on Rac1-deficient SST CINs

Another critical aspect of CIN maturation revolves around the formation of synapses. In our investigation, we assessed synapse density by analyzing the co-localization of prominent pre- and post-synaptic markers. Immunocytochemical data revealed a significant reduction in inhibitory synapses on both the soma and primary dendrites of SST CINs in vitro. Additionally, there was a noteworthy decrease in the number of excitatory synapses on SST CINs as well.

In a separate study, the selective removal of Rac1 from MGE-derived CINs led to a developmental reduction in inhibitory activity. This reduction in inhibitory activity, in turn, brought about functional alterations in cortical network activity within the adult mouse barrel cortex [96]. These alterations encompassed heightened synaptic transmission, a lowered threshold for stimulus-induced epileptiform activity, and disorganized oscillatory activity in brain slices. Among the observed irregularities in oscillatory activity were modifications in the gamma frequency range.

The decrease in CINs within the cortex, as well as the heightened synaptic transmission and network asynchrony, align with our findings of reduced inhibitory synapse density on SST CINs. These collective observations underscore the intricate relationship between Rac1 and the development and functioning of cortical inhibitory interneurons [58,95,96].

Reduced Potentiation in CNTN2/TAG1 Knock-out

In this experiment, we investigated the induction and maintenance of Long-Term Potentiation (LTP) in the hippocampal CA1 area using CNTN2/TAG-1 KO (DT-A -; TAG1 -/-) and WT (DT-A -; TAG1 +/+) mice. Our results, as illustrated in Figure 8, revealed a striking difference in LTP response between the two groups.

Specifically, the KO animals exhibited a decreased LTP response, which closely resembled the baseline recordings obtained before the theta-burst stimulation. In contrast, the WT mice displayed an expected increase in response, evident in the elevated percentage of fEPSPs peak and the corresponding traces.

This intriguing divergence in LTP response can be attributed to two plausible explanations. First, it is possible that the decreased LTP response in the CNTN2/TAG-1 KO animals results from an upregulation of excitation within the SST interneurons. This, in turn, could enhance the inhibition of pyramidal neurons, which are the primary targets of SST interneurons. This mechanism suggests a complex interplay between inhibitory and excitatory pathways that may be altered in the absence of CNTN2/TAG-1.

Alternatively, our results also raise the possibility of differences in NMDA receptors between CNTN2/TAG-1 WT and KO animals. Such variations in NMDA receptor function could contribute to the observed decrease in LTP response following theta-burst stimulation.

In conclusion, our findings highlight the critical role of CNTN2/TAG-1 in modulating LTP in the hippocampal CA1 area. The observed alterations in LTP response in KO animals suggest intricate interactions involving both inhibitory interneurons and NMDA receptors. Further investigations are warranted to elucidate the precise mechanisms underlying these intriguing observations and their implications for synaptic plasticity and neural circuit function.

Future Experiments

Considering the strong connectivity between pyramidal cells and SST-expressing interneurons, it would be highly informative to investigate potential alterations in synapses on pyramidal cells in Rac1cKO mice. Such insights could be obtained through in vitro or in vivo studies, employing techniques like immunocytochemistry (ICC) or immunohistochemistry (IHC), respectively. These studies could utilize antibodies against a pyramidal marker, such as Emx1 or CaMKII, along with synaptic markers as employed in our present investigation.

To ascertain whether the observed defects in vitro translate to in vivo scenarios, we could perform intracranial injections of CRE-dependent TdTomato-expressing adeno-associated virus (AAV) into the cortices of Rac1 mutant mice and their control littermates(Rac1 -/-; Nkx2.1 +/Cre) at postnatal days 0 to 2 (P0-P2). A similar approach was previously employed in our research regarding PV CINs. Unfortunately, due to the limited supply of Rac1-/-; Cre+/- mice, we

were unable to standardize and execute these experiments within the current study.There was some attempts but there was an issue with the AAV as it couldn't mark the CRE expressing interneurons with TdTomato. A solution to that could be to reduce the concentration of the virus, as the high concentration of the virus could affect the staining later, as it would not mark specifically.

Should we observe alterations in dendritic spines or synapse density in Rac1cKO mice in comparison to their control counterparts, the next step would involve exploring the functional properties of these neurons. To achieve this, we would employ whole-cell patch-clamp recordings in current-clamp mode. This would allow us to uncover any potential changes in intrinsic electrophysiological properties, encompassing passive properties (such as resting membrane potential and input resistance) and active properties (including action potential amplitude, rate of rise, and duration).

Finally, it is necessary to repeat the experiments with a greater animal population, at least n=3 for every condition. The results may have statistical significance but it was mainly due to the great number of SST+ CINs that was measured from each animal. Also, as the cell cultures between the WT and Rac1cKO were not of the same quality, there is a need to repeat the experiments to verify the results of the work. Probably this difference in the quality of the experiments between the two groups resulted from the experience this method requires as it is a method that needs hands-on experience. The cell cultures gradually became better and better with the last ones, which were the Rac1 KO, being the best as the cells were distributed evenly without becoming clumps of multiple cells and their neurites developed a well-made network connected the cells.Also, this might be a result of using B6 animals as control and not Rac1 +/+ ; Nkx2.1 +/Cre. This probably didn't affect the results but it is a factor that needs to be eliminated.

In conclusion, our findings underscore the pivotal role of Rac1 in interneuron development. It remains to be determined whether Rac1 directly governs the morphological and synaptic properties of SST+ CINs during their maturation or if its influence is mediated indirectly through specific downstream molecules. One potential avenue for further investigation involves analyzing data from RNA-sequencing and proteomic analyses conducted during early postnatal stages, comparing control and Rac1 cKO mice. Identification of differentially expressed molecules that interact with Rac1 and have known involvement in processes like dendritic arborization or synaptogenesis may shed light on the mechanisms underlying the observed defects in CIN maturation.

We anticipate that our findings will contribute significantly to unraveling the role of intracellular proteins, such as Rac1, in the mechanisms governing CIN development. This is a matter of considerable importance, particularly given the implication of CIN deficits in various diseases and the ongoing establishment of preclinical models for CIN-based cell therapies.

In the context of the second phase of our research project, we aimed to explore the influence of TAG-1/CNTN-2 on the excitability of SST+ interneurons. While this has provided valuable insights, it has also opened the door to a series of prospective experiments.

Firstly, we intend to extend our immunohistochemical investigations to comprehensively examine the myelination patterns of SST+ interneurons in TAG-1/CNTN-2 KO and WT animals. This continued examination will offer a more detailed understanding of the impact of TAG-1/CNTN-2 on the myelination process of these interneurons.

Furthermore, our research will delve deeper into the electrophysiological properties of SST+ CINs by employing whole-cell patch-clamp recordings. This approach will enable us to precisely quantify how the absence of TAG-1/CNTN-2 affects the electrophysiological behavior of these interneurons, shedding light on the functional consequences of the observed changes.

Additionally, our investigation will extend to explore potential effects on Long-Term Depression (LTD) recordings between TAG-1/CNTN-2 KO and WT animals. This experiment will further our understanding of the role of TAG-1/CNTN-2 in synaptic plasticity, particularly with regard to LTD.

These future experiments will collectively contribute to a more comprehensive and nuanced understanding of the functional significance of TAG-1/CNTN-2 in the context of SST+ interneurons, myelination, electrophysiological properties, and synaptic plasticity. The outcomes of these investigations hold the potential to unveil critical insights into the molecular mechanisms underpinning neural circuit function and plasticity.

References

1. Marín, O. & Rubenstein, J. L. R. Cell migration in the forebrain. *Annu. Rev. Neurosci.* **26**, 441–483 (2003).
2. Marín, O. Interneuron dysfunction in psychiatric disorders. *Nat. Rev. Neurosci.* **13**, 107–120 (2012).
3. Lunden, J. W., Durens, M., Phillips, A. W. & Nestor, M. W. Cortical interneuron function in autism spectrum condition. *Pediatr. Res.* **85**, 146–154 (2019).
4. Lewis, D. A., Hashimoto, T. & Volk, D. W. Cortical inhibitory neurons and schizophrenia. *Nat. Rev. Neurosci.* **6**, 312–324 (2005).
5. Butt, S. J. B. *et al.* Transcriptional regulation of cortical interneuron development. *J. Neurosci.* **27**, 11847–11850 (2007).
6. Flames, N. *et al.* Delineation of multiple subpallial progenitor domains by the combinatorial expression of transcriptional codes. *J. Neurosci.* **27**, 9682–9695 (2007).
7. Ascoli, G. A. & Samsonovich, A. V. Science of the conscious mind. *Biol. Bull.* **215**, 204–215 (2008).
8. DeFelipe, J. *et al.* New insights into the classification and nomenclature of cortical GABAergic interneurons. *Nat. Rev. Neurosci.* **14**, 202–216 (2013).
9. Lim, L., Mi, D., Llorca, A. & Marín, O. Development and Functional Diversification of Cortical Interneurons. *Neuron* **100**, 294–313 (2018).
10. Tremblay, R., Lee, S. & Rudy, B. GABAergic Interneurons in the Neocortex: From Cellular Properties to Circuits. *Neuron* **91**, 260–292 (2016).
11. Inan, M., Welagen, J. & Anderson, S. A. Spatial and temporal bias in the mitotic origins of somatostatin- and parvalbumin-expressing interneuron subgroups and the chandelier subtype in the medial ganglionic eminence. *Cereb. Cortex* **22**, 820–827 (2012).
12. Taniguchi, H., Lu, J. & Huang, Z. J. The spatial and temporal origin of chandelier cells in mouse neocortex. *Science* **339**, 70–74 (2013).

13. Cardin, J. A. *et al.* Driving fast-spiking cells induces gamma rhythm and controls sensory responses. *Nature* **459**, 663–667 (2009).
14. Hormuzdi, S. G. *et al.* Impaired electrical signaling disrupts gamma frequency oscillations in connexin 36-deficient mice. *Neuron* **31**, 487–495 (2001).
15. Sohal, V. S., Zhang, F., Yizhar, O. & Deisseroth, K. Parvalbumin neurons and gamma rhythms enhance cortical circuit performance. *Nature* **459**, 698–702 (2009).
16. Gonzalez-Burgos, G., Cho, R. Y. & Lewis, D. A. Alterations in cortical network oscillations and parvalbumin neurons in schizophrenia. *Biol. Psychiatry* **77**, 1031–1040 (2015).
17. Hu, H., Gan, J. & Jonas, P. Interneurons. Fast-spiking, parvalbumin^{+} GABAergic interneurons: from cellular design to microcircuit function. *Science* **345**, 1255263 (2014).
18. Somogyi, P., Freund, T. F. & Cowey, A. The axo-axonic interneuron in the cerebral cortex of the rat, cat and monkey. *Neuroscience* **7**, 2577–2607 (1982).
19. Bortone, D. S., Olsen, S. R. & Scanziani, M. Translaminar inhibitory cells recruited by layer 6 corticothalamic neurons suppress visual cortex. *Neuron* **82**, 474–485 (2014).
20. Buchanan, K. A. *et al.* Target-specific expression of presynaptic NMDA receptors in neocortical microcircuits. *Neuron* **75**, 451–466 (2012).
21. Hilscher, M. M., Leão, R. N., Edwards, S. J., Leão, K. E. & Kullander, K. Chrna2-Martinotti Cells Synchronize Layer 5 Type A Pyramidal Cells via Rebound Excitation. *PLoS Biol.* **15**, e2001392 (2017).
22. Wang, Y. *et al.* Anatomical, physiological and molecular properties of Martinotti cells in the somatosensory cortex of the juvenile rat. *J. Physiol.* **561**, 65–90 (2004).
23. Xu, X., Roby, K. D. & Callaway, E. M. Mouse cortical inhibitory neuron type that coexpresses somatostatin and calretinin. *J. Comp. Neurol.* **499**, 144–160 (2006).
24. Jiang, X. *et al.* Principles of connectivity among morphologically defined cell types in adult neocortex. *Science* **350**, aac9462 (2015).
25. Nigro, M. J., Hashikawa-Yamasaki, Y. & Rudy, B. Diversity and Connectivity of Layer 5 Somatostatin-Expressing Interneurons in the Mouse Barrel Cortex. *J. Neurosci.* **38**, 1622–1633 (2018).
26. Silberberg, G. & Markram, H. Disynaptic inhibition between neocortical pyramidal cells mediated by Martinotti cells. *Neuron* **53**, 735–746 (2007).
27. Xu, H., Jeong, H.-Y., Tremblay, R. & Rudy, B. Neocortical somatostatin-expressing GABAergic interneurons disinhibit the thalamorecipient layer 4. *Neuron* **77**, 155–167 (2013).
28. Kawaguchi, Y. & Kubota, Y. Neurochemical features and synaptic connections of large physiologically-identified GABAergic cells in the rat frontal cortex. *Neuroscience* **85**, 677–701 (1998).
29. Oláh, S. *et al.* Output of neurogliaform cells to various neuron types in the human and rat cerebral cortex. *Front. Neural Circuits* **1**, 4 (2007).
30. Tasic, B. *et al.* Shared and distinct transcriptomic cell types across neocortical areas. *Nature* **563**, 72–78 (2018).
31. Frazer, S. *et al.* Transcriptomic and anatomic parcellation of 5-HTR expressing cortical interneuron subtypes revealed by single-cell RNA sequencing. *Nat. Commun.* **8**, 14219 (2017).
32. Gelman, D. M. *et al.* The embryonic preoptic area is a novel source of cortical GABAergic

interneurons. *J. Neurosci.* **29**, 9380–9389 (2009).
33. Miyoshi, G. *et al.* Genetic fate mapping reveals that the caudal ganglionic eminence produces a large and diverse population of superficial cortical interneurons. *J. Neurosci.* **30**, 1582–1594 (2010).
34. Anderson, S. A., Eisenstat, D. D., Shi, L. & Rubenstein, J. L. Interneuron migration from basal forebrain to neocortex: dependence on Dlx genes. *Science* **278**, 474–476 (1997).
35. Marín, O. & Rubenstein, J. L. A long, remarkable journey: tangential migration in the telencephalon. *Nat. Rev. Neurosci.* **2**, 780–790 (2001).
36. Wamsley, B. & Fishell, G. Genetic and activity-dependent mechanisms underlying interneuron diversity. *Nat. Rev. Neurosci.* **18**, 299–309 (2017).
37. Hansen, D. V. *et al.* Non-epithelial stem cells and cortical interneuron production in the human ganglionic eminences. *Nat. Neurosci.* **16**, 1576–1587 (2013).
38. Ma, T. *et al.* Subcortical origins of human and monkey neocortical interneurons. *Nat. Neurosci.* **16**, 1588–1597 (2013).
39. Gelman, D. M. & Marín, O. Generation of interneuron diversity in the mouse cerebral cortex. *Eur. J. Neurosci.* **31**, 2136–2141 (2010).
40. Butt, S. J. B. *et al.* The requirement of Nkx2-1 in the temporal specification of cortical interneuron subtypes. *Neuron* **59**, 722–732 (2008).
41. Gelman, D. *et al.* A wide diversity of cortical GABAergic interneurons derives from the embryonic preoptic area. *J. Neurosci.* **31**, 16570–16580 (2011).
42. Lavdas, A. A., Grigoriou, M., Pachnis, V. & Parnavelas, J. G. The medial ganglionic eminence gives rise to a population of early neurons in the developing cerebral cortex. *J. Neurosci.* **19**, 7881–7888 (1999).
43. Wichterle, H., Turnbull, D. H., Nery, S., Fishell, G. & Alvarez-Buylla, A. In utero fate mapping reveals distinct migratory pathways and fates of neurons born in the mammalian basal forebrain. *Development* **128**, 3759–3771 (2001).
44. Xu, Q., Cobos, I., De La Cruz, E., Rubenstein, J. L. & Anderson, S. A. Origins of cortical interneuron subtypes. *J. Neurosci.* **24**, 2612–2622 (2004).
45. Xu, Q., Tam, M. & Anderson, S. A. Fate mapping Nkx2.1-lineage cells in the mouse telencephalon. *J. Comp. Neurol.* **506**, 16–29 (2008).
46. Sultan, K. T., Brown, K. N. & Shi, S.-H. Production and organization of neocortical interneurons. *Front. Cell. Neurosci.* **7**, 221 (2013).
47. Wonders, C. P. & Anderson, S. A. The origin and specification of cortical interneurons. *Nat. Rev. Neurosci.* **7**, 687–696 (2006).
48. Métin, C., Baudoin, J.-P., Rakić, S. & Parnavelas, J. G. Cell and molecular mechanisms involved in the migration of cortical interneurons. *Eur. J. Neurosci.* **23**, 894–900 (2006).
49. Sussel, L., Marin, O., Kimura, S. & Rubenstein, J. L. Loss of Nkx2.1 homeobox gene function results in a ventral to dorsal molecular respecification within the basal telencephalon: evidence for a transformation of the pallidum into the striatum. *Development* **126**, 3359–3370 (1999).
50. Martini, F. J. *et al.* Biased selection of leading process branches mediates chemotaxis during tangential neuronal migration. *Development* **136**, 41–50 (2009).
51. Moll, J., Sansig, G., Fattori, E. & van der Putten, H. The murine rac1 gene: cDNA cloning, tissue distribution and regulated expression of rac1 mRNA by disassembly of actin

microfilaments. *Oncogene* **6**, 863–866 (1991).
52. Malosio, M. L., Gilardelli, D., Paris, S., Albertinazzi, C. & de Curtis, I. Differential expression of distinct members of Rho family GTP-binding proteins during neuronal development: identification of Rac1B, a new neural-specific member of the family. *J. Neurosci.* **17**, 6717–6728 (1997).
53. Watabe-Uchida, M., John, K. A., Janas, J. A., Newey, S. E. & Van Aelst, L. The Rac activator DOCK7 regulates neuronal polarity through local phosphorylation of stathmin/Op18. *Neuron* **51**, 727–739 (2006).
54. Jaffe, A. B. & Hall, A. Rho GTPases: biochemistry and biology. *Annu. Rev. Cell Dev. Biol.* **21**, 247–269 (2005).
55. Govek, E.-E., Newey, S. E. & Van Aelst, L. The role of the Rho GTPases in neuronal development. *Genes Dev.* **19**, 1–49 (2005).
56. Ramakers, G. J. A. Rho proteins, mental retardation and the cellular basis of cognition. *Trends Neurosci.* **25**, 191–199 (2002).
57. Kholmanskikh, S. S., Dobrin, J. S., Wynshaw-Boris, A., Letourneau, P. C. & Ross, M. E. Disregulated RhoGTPases and actin cytoskeleton contribute to the migration defect in Lis1-deficient neurons. *J. Neurosci.* **23**, 8673–8681 (2003).
58. Vidaki, M. *et al.* Rac1-dependent cell cycle exit of MGE precursors and GABAergic interneuron migration to the cortex. *Cereb. Cortex* **22**, 680–692 (2012).
59. Tahirovic, S. *et al.* Rac1 regulates neuronal polarization through the WAVE complex. *J. Neurosci.* **30**, 6930–6943 (2010).
60. Gualdoni, S., Albertinazzi, C., Corbetta, S., Valtorta, F. & de Curtis, I. Normal levels of Rac1 are important for dendritic but not axonal development in hippocampal neurons. *Biol. Cell* **99**, 455–464 (2007).
61. Cingolani, L. A. & Goda, Y. Actin in action: the interplay between the actin cytoskeleton and synaptic efficacy. *Nat. Rev. Neurosci.* **9**, 344–356 (2008).
62. Luo, L. Actin cytoskeleton regulation in neuronal morphogenesis and structural plasticity. *Annu. Rev. Cell Dev. Biol.* **18**, 601–635 (2002).
63. Ethell, I. M. & Pasquale, E. B. Molecular mechanisms of dendritic spine development and remodeling. *Prog. Neurobiol.* **75**, 161–205 (2005).
64. Tada, T. & Sheng, M. Molecular mechanisms of dendritic spine morphogenesis. *Curr. Opin. Neurobiol.* **16**, 95–101 (2006).
65. Schubert, V. & Dotti, C. G. Transmitting on actin: synaptic control of dendritic architecture. *J. Cell Sci.* **120**, 205–212 (2007).
66. Halpain, S. Actin and the agile spine: how and why do dendritic spines dance? *Trends Neurosci.* **23**, 141–146 (2000).
67. Renner, M., Specht, C. G. & Triller, A. Molecular dynamics of postsynaptic receptors and scaffold proteins. *Curr. Opin. Neurobiol.* **18**, 532–540 (2008).
68. Sheng, M. & Hoogenraad, C. C. The postsynaptic architecture of excitatory synapses: a more quantitative view. *Annu. Rev. Biochem.* **76**, 823–847 (2007).
69. Pennucci, R., Gucciardi, I. & de Curtis, I. Rac1 and Rac3 GTPases differently influence the morphological maturation of dendritic spines in hippocampal neurons. *PLoS One* **14**, e0220496 (2019).
70. Bourne, J. N. & Harris, K. M. Nanoscale analysis of structural synaptic plasticity. *Curr. Opin.*

Neurobiol. **22**, 372–382 (2012).
71. van Bommel, B., Konietzny, A., Kobler, O., Bär, J. & Mikhaylova, M. F-actin patches associated with glutamatergic synapses control positioning of dendritic lysosomes. *EMBO J.* **38**, e101183 (2019).
72. Liu, Y. & Edwards, R. H. The role of vesicular transport proteins in synaptic transmission and neural degeneration. *Annu. Rev. Neurosci.* **20**, 125–156 (1997).
73. Bucher, M., Fanutza, T. & Mikhaylova, M. Cytoskeletal makeup of the synapse: Shaft versus spine. *Cytoskeleton* **77**, 55–64 (2020).
74. Verstraelen, P. *et al.* Systematic Quantification of Synapses in Primary Neuronal Culture. *iScience* **23**, 101542 (2020).
75. Anggono, V. & Huganir, R. L. Regulation of AMPA receptor trafficking and synaptic plasticity. *Curr. Opin. Neurobiol.* **22**, 461–469 (2012).
76. Geiger, J. C. *et al.* The GRIP1/14-3-3 pathway coordinates cargo trafficking and dendrite development. *Dev. Cell* **28**, 381–393 (2014).
77. Hruska, M., Henderson, N., Le Marchand, S. J., Jafri, H. & Dalva, M. B. Synaptic nanomodules underlie the organization and plasticity of spine synapses. *Nat. Neurosci.* **21**, 671–682 (2018).
78. MacGillavry, H. D., Song, Y., Raghavachari, S. & Blanpied, T. A. Nanoscale scaffolding domains within the postsynaptic density concentrate synaptic AMPA receptors. *Neuron* **78**, 615–622 (2013).
79. Cesca, F., Baldelli, P., Valtorta, F. & Benfenati, F. The synapsins: key actors of synapse function and plasticity. *Prog. Neurobiol.* **91**, 313–348 (2010).
80. Chiu, C. Q. *et al.* Compartmentalization of GABAergic inhibition by dendritic spines. *Science* **340**, 759–762 (2013).
81. Jacob, T. C., Moss, S. J. & Jurd, R. GABA(A) receptor trafficking and its role in the dynamic modulation of neuronal inhibition. *Nat. Rev. Neurosci.* **9**, 331–343 (2008).
82. Tyagarajan, S. K. & Fritschy, J.-M. Gephyrin: a master regulator of neuronal function? *Nat. Rev. Neurosci.* **15**, 141–156 (2014).
83. Choii, G. & Ko, J. Gephyrin: a central GABAergic synapse organizer. *Exp. Mol. Med.* **47**, e158 (2015).
84. Alvarez, F. J. Gephyrin and the regulation of synaptic strength and dynamics at glycinergic inhibitory synapses. *Brain Res. Bull.* **129**, 50–65 (2017).
85. Groeneweg, F. L., Trattnig, C., Kuhse, J., Nawrotzki, R. A. & Kirsch, J. Gephyrin: a key regulatory protein of inhibitory synapses and beyond. *Histochem. Cell Biol.* **150**, 489–508 (2018).
86. Chaudhry, F. A. *et al.* The vesicular GABA transporter, VGAT, localizes to synaptic vesicles in sets of glycinergic as well as GABAergic neurons. *J. Neurosci.* **18**, 9733–9750 (1998).
87. McIntire, S. L., Reimer, R. J., Schuske, K., Edwards, R. H. & Jorgensen, E. M. Identification and characterization of the vesicular GABA transporter. *Nature* **389**, 870–876 (1997).
88. Fishell, G. & Rudy, B. Mechanisms of inhibition within the telencephalon: ‘where the wild things are’. *Annu. Rev. Neurosci.* **34**, 535–567 (2011).
89. Molyneaux, B. J., Arlotta, P., Menezes, J. R. L. & Macklis, J. D. Neuronal subtype specification in the cerebral cortex. *Nat. Rev. Neurosci.* **8**, 427–437 (2007).
90. Canitano, R. & Pallagrosi, M. Autism Spectrum Disorders and Schizophrenia Spectrum

Disorders: Excitation/Inhibition Imbalance and Developmental Trajectories. *Front. Psychiatry* **8**, 69 (2017).
91. Fung, S. J., Fillman, S. G., Webster, M. J. & Shannon Weickert, C. Schizophrenia and bipolar disorder show both common and distinct changes in cortical interneuron markers. *Schizophr. Res.* **155**, 26–30 (2014).
92. Gao, R. & Penzes, P. Common mechanisms of excitatory and inhibitory imbalance in schizophrenia and autism spectrum disorders. *Curr. Mol. Med.* **15**, 146–167 (2015).
93. Luscher, B., Shen, Q. & Sahir, N. The GABAergic deficit hypothesis of major depressive disorder. *Mol. Psychiatry* **16**, 383–406 (2011).
94. Selten, M., van Bokhoven, H. & Nadif Kasri, N. Inhibitory control of the excitatory/inhibitory balance in psychiatric disorders. *F1000Res.* **7**, 23 (2018).
95. Konstantoudaki, X., Chalkiadaki, K., Tivodar, S., Karagogeos, D. & Sidiropoulou, K. Impaired synaptic plasticity in the prefrontal cortex of mice with developmentally decreased number of interneurons. *Neuroscience* **322**, 333–345 (2016).
96. Kalemaki, K., Konstantoudaki, X., Tivodar, S., Sidiropoulou, K. & Karagogeos, D. Mice With Decreased Number of Interneurons Exhibit Aberrant Spontaneous and Oscillatory Activity in the Cortex. *Front. Neural Circuits* **12**, 96 (2018).
97. Habermacher, C., Angulo, M. C. & Benamer, N. Glutamate versus GABA in neuron-oligodendroglia communication. *Glia* **67**, 2092–2106 (2019).
98. Kessaris, N. *et al.* Competing waves of oligodendrocytes in the forebrain and postnatal elimination of an embryonic lineage. *Nat. Neurosci.* **9**, 173–179 (2006).
99. Micheva, K. D. *et al.* A large fraction of neocortical myelin ensheathes axons of local inhibitory neurons. *Elife* **5**, (2016).
100. Balia, M., Benamer, N. & Angulo, M. C. A specific GABAergic synapse onto oligodendrocyte precursors does not regulate cortical oligodendrogenesis. *Glia* **65**, 1821–1832 (2017).
101. Fields, R. D. White matter in learning, cognition and psychiatric disorders. *Trends Neurosci.* **31**, 361–370 (2008).
102. Ruden, J. B., Dugan, L. L. & Konradi, C. Parvalbumin interneuron vulnerability and brain disorders. *Neuropsychopharmacology* **46**, 279–287 (2021).
103. Stedehouder, J. *et al.* Fast-spiking Parvalbumin Interneurons are Frequently Myelinated in the Cerebral Cortex of Mice and Humans. *Cereb. Cortex* **27**, 5001–5013 (2017).
104. Bonetto, G. *et al.* Selective Axonal Expression of the Kv1 Channel Complex in Pre-myelinated GABAergic Hippocampal Neurons. *Front. Cell. Neurosci.* **13**, 222 (2019).
105. Huxley, A. F. & Stampfli, R. Evidence for saltatory conduction in peripheral myelinated nerve fibres. *J. Physiol.* **108**, 315–339 (1949).
106. Saab, A. S. *et al.* Oligodendroglial NMDA Receptors Regulate Glucose Import and Axonal Energy Metabolism. *Neuron* **91**, 119–132 (2016).
107. Pellerin, L. & Magistretti, P. J. Glutamate uptake into astrocytes stimulates aerobic glycolysis: a mechanism coupling neuronal activity to glucose utilization. *Proc. Natl. Acad. Sci. U. S. A.* **91**, 10625–10629 (1994).
108. Bechler, M. E., Byrne, L. & Ffrench-Constant, C. CNS Myelin Sheath Lengths Are an Intrinsic Property of Oligodendrocytes. *Curr. Biol.* **25**, 2411–2416 (2015).
109. Bechler, M. E., Swire, M. & Ffrench-Constant, C. Intrinsic and adaptive myelination-A

sequential mechanism for smart wiring in the brain. *Dev. Neurobiol.* **78**, 68–79 (2018).
110. Ghosh, A., Sherman, D. L. & Brophy, P. J. The Axonal Cytoskeleton and the Assembly of Nodes of Ranvier. *Neuroscientist* **24**, 104–110 (2018).
111. Yermakov, L. M., Hong, L. A., Drouet, D. E., Griggs, R. B. & Susuki, K. Functional Domains in Myelinated Axons. *Adv. Exp. Med. Biol.* **1190**, 65–83 (2019).
112. Kalafatakis, I., Savvaki, M., Velona, T. & Karagogeos, D. Implication of Contactins in Demyelinating Pathologies. *Life* **11**, (2021).
113. Walmsley, M. J. *et al.* Critical roles for Rac1 and Rac2 GTPases in B cell development and signaling. *Science* **302**, 459–462 (2003).
114. Fogarty, M. *et al.* Spatial genetic patterning of the embryonic neuroepithelium generates GABAergic interneuron diversity in the adult cortex. *J. Neurosci.* **27**, 10935–10946 (2007).
115. Srinivas, S. *et al.* Cre reporter strains produced by targeted insertion of EYFP and ECFP into the ROSA26 locus. *BMC Dev. Biol.* **1**, 4 (2001).
116. Fukamauchi, F. *et al.* TAG-1-deficient mice have marked elevation of adenosine A1 receptors in the hippocampus. *Biochem. Biophys. Res. Commun.* **281**, 220–226 (2001).
117. Dzyubenko, E., Rozenberg, A., Hermann, D. M. & Faissner, A. Colocalization of synapse marker proteins evaluated by STED-microscopy reveals patterns of neuronal synapse distribution in vitro. *J. Neurosci. Methods* **273**, 149–159 (2016).
118. Merchán-Pérez, A. *et al.* Three-dimensional spatial distribution of synapses in the neocortex: a dual-beam electron microscopy study. *Cereb. Cortex* **24**, 1579–1588 (2014).
119. Conde, C. & Cáceres, A. Microtubule assembly, organization and dynamics in axons and dendrites. *Nat. Rev. Neurosci.* **10**, 319–332 (2009).
120. Stiess, M. & Bradke, F. Neuronal polarization: the cytoskeleton leads the way. *Dev. Neurobiol.* **71**, 430–444 (2011).